Mississippian Barnett Shale: Lithofacies and depositional setting of a deep-water shale-gas succession in the Fort Worth Basin, Texas

Robert G. Loucks and Stephen C. Ruppel

ABSTRACT

The Mississippian Barnett Formation of the Fort Worth Basin is a classic shale-gas system in which the rock is the source, reservoir, and seal. Barnett strata were deposited in a deeper water foreland basin that had poor circulation with the open ocean. For most of the basin's history, bottom waters were euxinic, preserving organic matter and, thus, creating a rich source rock, along with abundant framboidal pyrite. The Barnett interval comprises a variety of facies but is dominated by fine-grained (clay- to silt-size) particles. Three general lithofacies are recognized on the basis of mineralogy, fabric, biota, and texture: (1) laminated siliceous mudstone; (2) laminated argillaceous lime mudstone (marl); and (3) skeletal, argillaceous lime packstone. Each facies contains abundant pyrite and phosphate (apatite), which are especially common at hardgrounds. Carbonate concretions, a product of early diagenesis, are also common. The entire Barnett biota is composed of debris transported to the basin from the shelf or upper oxygenated slope by hemipelagic mud plumes, dilute turbidites, and debris flows. Biogenic sediment was also sourced from the shallower, better oxygenated water column. Barnett deposition is estimated to have occurred over a 25-m.y. period, and despite the variations in sublithofacies, sedimentation style remained remarkably similar throughout this span of time.

INTRODUCTION

The Mississippian Barnett Shale of the Fort Worth Basin (FWB) (Figure 1) is a shale-gas system (Curtis, 2002) composed of a mixture of laminated siliceous mudstone, laminated argillaceous lime

Manuscript received May 30, 2006; provisional acceptance August 22, 2006; revised manuscript received September 27, 2006; final acceptance November 2, 2006.
DOI:10.1306/11020606059

AUTHORS

ROBERT G. LOUCKS ~ *Bureau of Economic Geology, John A. and Catherine G. Jackson School of Geosciences, University of Texas at Austin, 10100 Bureau Road, Building 130, Austin, Texas 78713-8924; bob.loucks@beg.utexas.edu*

Robert Loucks is a senior research scientist at the Bureau of Economic Geology. He received his B.A. degree from the State University of New York at Binghamton in 1967 and his Ph.D. from the University of Texas at Austin in 1976. His general research interests include carbonate and siliciclastic sequence stratigraphy, depositional systems, diagenesis, and reservoir characterization. His present research is focused on shale-gas systems.

STEPHEN C. RUPPEL ~ *Bureau of Economic Geology, John A. and Catherine G. Jackson School of Geosciences, University of Texas at Austin, 10100 Bureau Road, Building 130, Austin, Texas 78713-8924*

Stephen Ruppel has studied the stratigraphy of Paleozoic carbonate successions for nearly 30 years. He holds a Ph.D. from the University of Tennessee, Knoxville, and is currently a senior research scientist at the Bureau of Economic Geology. In addition to the Barnett shale-gas studies, he maintains active research interests in the complete Paleozoic carbonate section of the Permian Basin.

ACKNOWLEDGEMENTS

We thank the following people for valuable discussions on the geology of the Barnett Formation: Wayne Wright, Kitty Milliken, Rob Reed, Dan Jarvie, and Alton Brown. Dan Jarvie also kindly supplied us with total organic carbon data from several cores. Rob Reed provided several scanning electron microscopy photographs. Ronald Hill and Berry Tew, Jr., provided reviews of the manuscript for AAPG. We appreciate their strong effort to improve the article. Lana Dieterich at the Bureau of Economic Geology edited the article. We thank the Geology Foundation of the John A. and Katherine G. Jackson School of Geosciences at the University of Texas at Austin for providing funds for page charges. This publication is authorized by the director of the Bureau of Economic Geology.

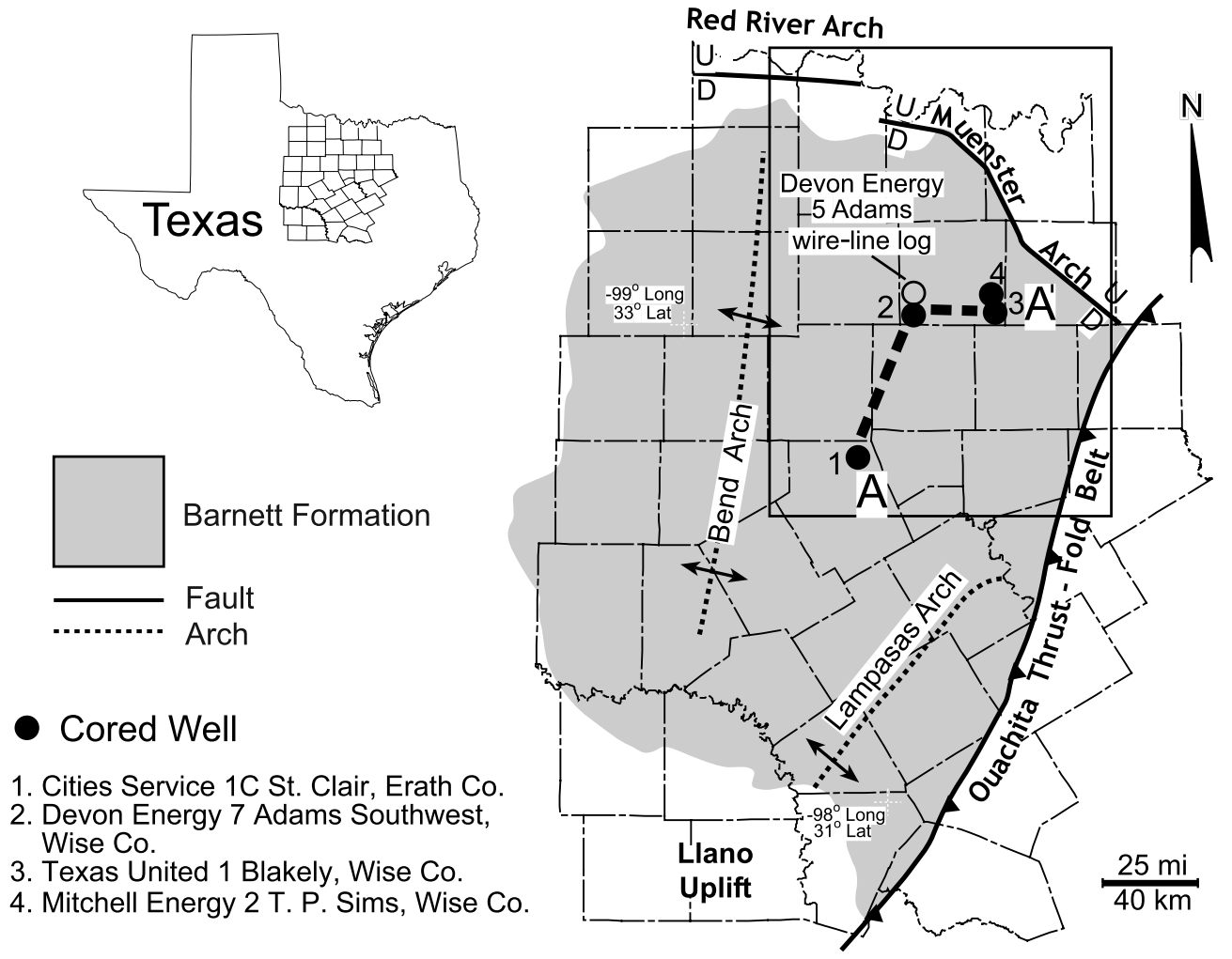

Figure 1. Map of the FWB showing the distribution of the Barnett Formation, general structural features, location of cores, and regional cross section. Map modified from Montgomery et al. (2005).

mudstone (marl), and skeletal argillaceous lime packstones. Newark East field, the largest gas field in Texas (Durham, 2005; Montgomery et al., 2005), is developed in this Barnett shale-gas system. The Barnett Formation continues to be an active target for shale gas in the FWB, as well as in the adjacent Permian Basin; age-equivalent rocks are also being explored in other states (Brown, 2006; Williams, 2006). Much effort has been devoted to understanding exploration methods, completion techniques, organic content, and maturation in this system. However, little has been published on the sedimentology, lithofacies, or depositional setting of these rocks. Bowker (2002), Gonzalez (2004), and Montgomery et al. (2005) published general reviews on Barnett geology, and Papazis (2005) completed a petrographic analysis of the Barnett Formation.

Figure 2 depicts the stratigraphic setting of the Barnett Formation. Depending on location, the Barnett section is underlain by the Mississippian Chappel Limestone, Middle to Upper Ordovician Viola and Simpson carbonates, or the Lower Ordovician Ellenburger Group. In most of the basin, the Barnett strata rest on a major unconformity that spans at least 100 m.y. and is overlain by the Pennsylvanian Marble Falls succession. The Barnett Formation can be divided into three members where the Forestburg limestone is present (Figure 2). Where this limestone is absent, the Barnett interval is treated generally as one unit (Montgomery et al., 2005).

Because of the importance of the Barnett Formation, we have undertaken an investigation of its lithofacies and depositional setting using core studies integrated with wire-line-log data. The major objectives of this investigation are to (1) define and describe the lithofacies and associated depositional and diagenetic features of the Barnett Formation and (2) define the conditions and setting in which the Barnett strata accumulated.

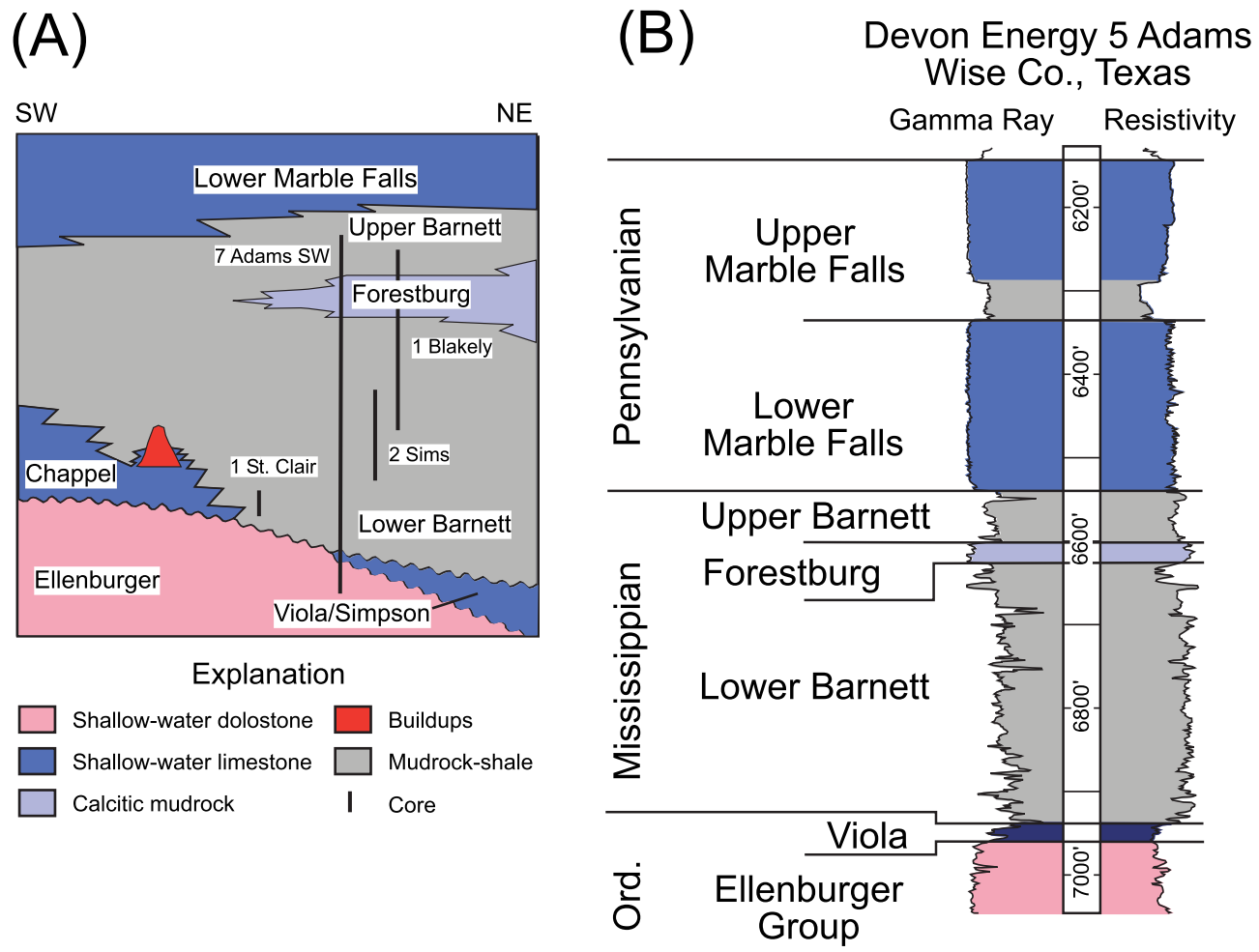

Figure 2. General stratigraphy of the Ordovician to Pennsylvanian section in the FWB. (A) Diagrammatic cross section of the stratigraphy of the Fort Basin after Montgomery et al. (2005). Approximate stratigraphic location of cores used in the study is shown. (B) Wire-line log with major stratigraphic units.

This report focuses on both depositional and diagenetic aspects of the Barnett Formation. Although studies of fractures, organic content and maturity, detailed paleontology, biostratigraphy, and geochronology are under way, they will be summarized in future reports.

METHODS

The key to our analysis of the Barnett interval is subsurface cores, four of which we described from the northern FWB (three from Wise County and one from Erath County) (Figures 1, 3). Three of the studied cores are stored at the Core Research Center, Bureau of Economic Geology, University of Texas at Austin, and were sampled for rock analysis. The fourth core, the Devon 7 Adams Southwest, was unavailable for sampling, although a detailed study of this core, complete with numerous core and thin-section photographs, was published by Papazis (2005). We have also made a preliminary study of outcrops and four additional cores available from counties in the southwest part of the FWB. Although not documented in detail in this article, these core and outcrop data provide important insights into the character and variability of the Barnett strata across the FWB. The general stratigraphy of the Barnett Formation and its component members is shown in Figures 2 and 3. Isopachs of the total Barnett section and the Forestburg limestone (Figure 4) were generated to define the geometry of the northern FWB.

Forty polished thin sections were prepared and analyzed for rock fabric, texture, biotic content, and mineralogy. Seventy high-resolution thin-section photographs were also available from Papazis (2005).

Thirty-one samples were analyzed by Omni Laboratory for mineralogy by x-ray diffraction (XRD) analysis.

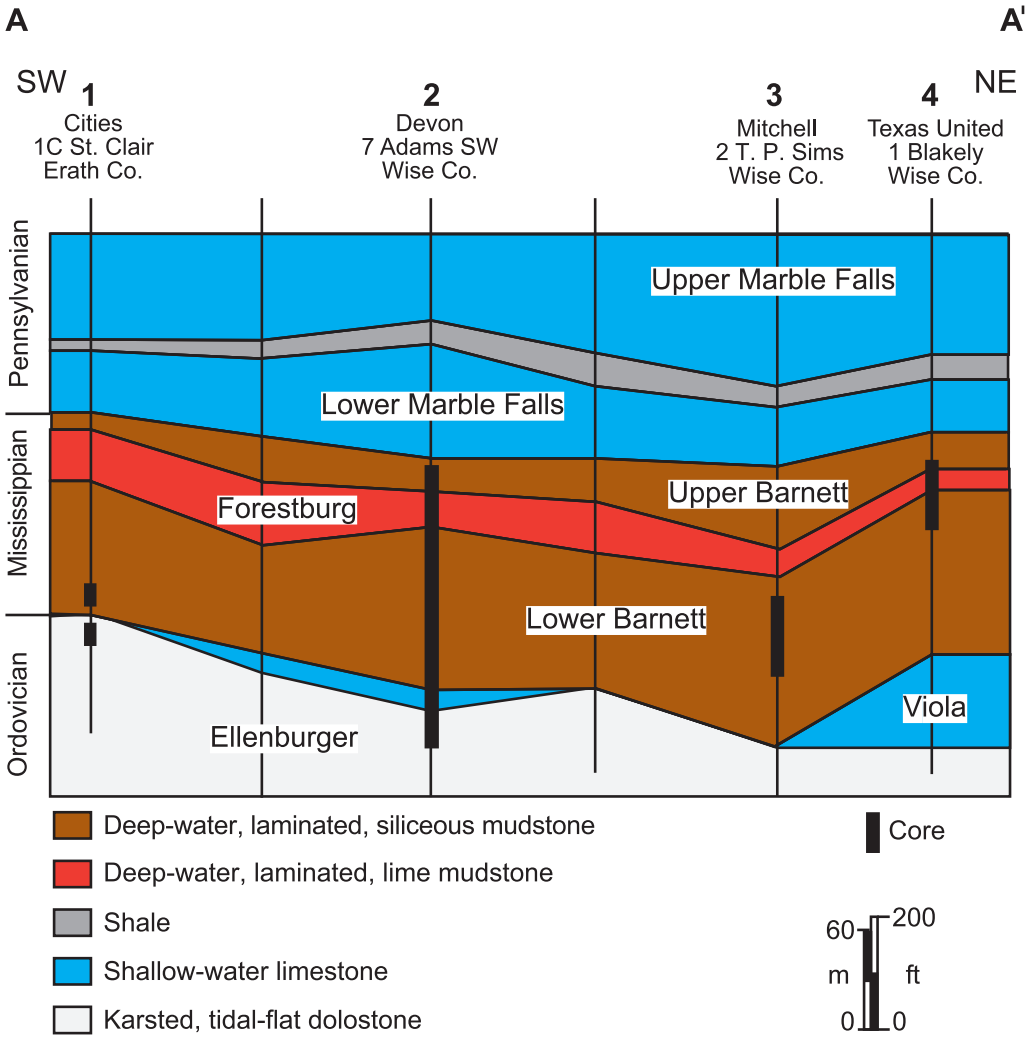

Figure 3. Cross section of cored wells showing general stratigraphy and lithofacies of Barnett and underlying and overlying units in the Wise County area.

Each sample was ground to a fine powder (10–15 μm). Bulk sample mounts were scanned with a Bruker AXS D4 Endeavor x-ray diffractometer using copper K-alpha radiation at standard scanning parameters. Computer analysis of the diffractograms provided identification and semiquantitative analysis of the relative abundance (in weight percent) of the various mineral phases.

PREVIOUS WORK

Turner (1957) published an excellent early summary of Paleozoic stratigraphy of the FWB. The U.S. Geological Survey study of the Mississippian section of the United States (Craig and Connor, 1979) includes a general analysis of Barnett thickness and facies patterns in the FWB. Henry (1982) provided a basic analysis of Barnett and underlying Chappel formations in the FWB area. Gutschick and Sandberg (1983) published a valuable analysis of the middle Osagean (lower Mississippian) section across the United States, primarily on the basis of their work in the western United States. Their models are applicable over much of the United States. Ruppel (1985) described thickness and facies variations in the Mississippian section in the Palo Duro and Hardeman basins and also published a general stratigraphic model for the Hardeman–FWB areas (Ruppel, 1989). More recently, Montgomery (2004) and Montgomery et al. (2005) published an extensive summary of the Barnett in the FWB.

REGIONAL SETTING

Understanding the shape and depth of the basin is complicated by the fact that the Ouachita thrust and fold belt have masked the basin's characteristics to the east and southeast (Figure 1). The Barnett section was eroded

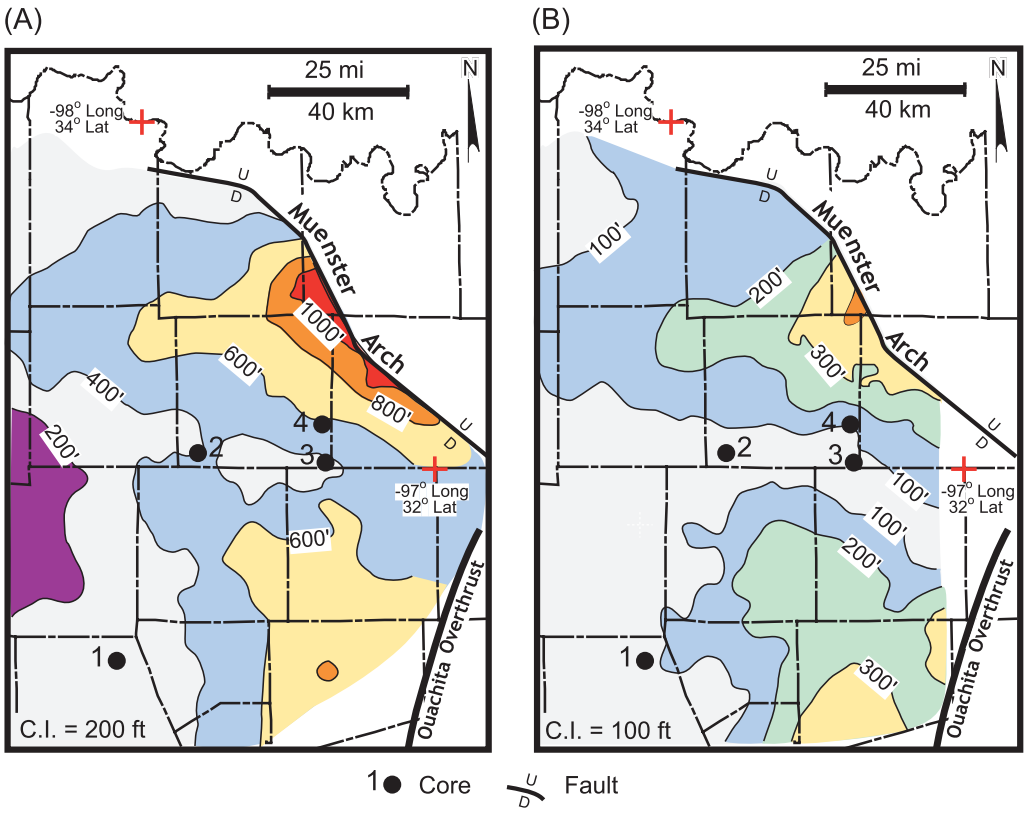

Figure 4. Isopach maps. (A) Isopach of total Barnett interval based on wire-line-log correlations. (B) Isopach of Forestburg interval based on wire-line-log correlations. Cored wells used in study are shown. See Figure 1 for well names.

during the Pennsylvanian from the Muenster arch area to the northeast (Montgomery et al., 2005).

As conventionally defined, the FWB is bounded on the west by the Bend arch, on the south by the Llano uplift, on the north by Pennsylvanian-age Red River and Muenster arches, and on the east by the Ouachita overthrust, also of Pennsylvanian age (Figure 1). Thickness variations in the Barnett Formation across the FWB are shown in Figure 4. It is apparent from preliminary core and wire-line-log studies, however, that Barnett strata extend farther west onto the Bend arch and into the area of the Llano uplift.

Global plate reconstructions by Blakey (2005) suggest that during the Mississippian, the FWB area occupied a narrow inland seaway between the rapidly approaching continents of Laurussia and Gondwana (Figure 5). This seaway was bounded on the west by a broad, shallow-water, carbonate shelf and on the east by an island arc chain. On the basis of their studies of the Mississippian in Nevada, Gutschick and Sandberg (1983) constructed a paleogeographic map of the western margin of the Laurussian paleocontinent during the Mississippian that depicts the distribution of shelf and basin areas and presumed water depths (Figure 6). Both of these reconstructions demonstrate that the FWB formed as a foreland basin on the leading (southern) edge of the Laurussian paleocontinent. Similar conclusions were reached by Arbenz (1989). The Mississippian Interior seaway extended along most of the southern and southeastern margins of the Laurussian paleocontinent (across the entire area of what is now the southern United States) (Figures 5, 6). Oceanic circulation within this seaway was probably restricted and may have accounted for the anoxic conditions indicated by the Barnett strata.

Dominant source areas for the FWB sediment during the Mississippian are the Chappel shelf to the west (which probably contributed mainly carbonate debris as hemipelagic plumes or as density flows down the slope) and the Caballos Arkansas island chain to the south (which probably contributed most of the terrigenous-derived clay- to silt-size sediment, such as quartz and feldspars, as plumes or density flows). Except for shell beds, most of the sediment in the northern FWB is silt size or smaller, indicating that no coarser grained, terrigenous-derived sediment was transported into the preserved FWB from the Caballos Arkansas island chain during the time of the Barnett deposition (Mississippian).

Water depths across the FWB are difficult to define precisely. Gutschick and Sandberg (1983) suggested water depths from 600 to more than 1000 ft

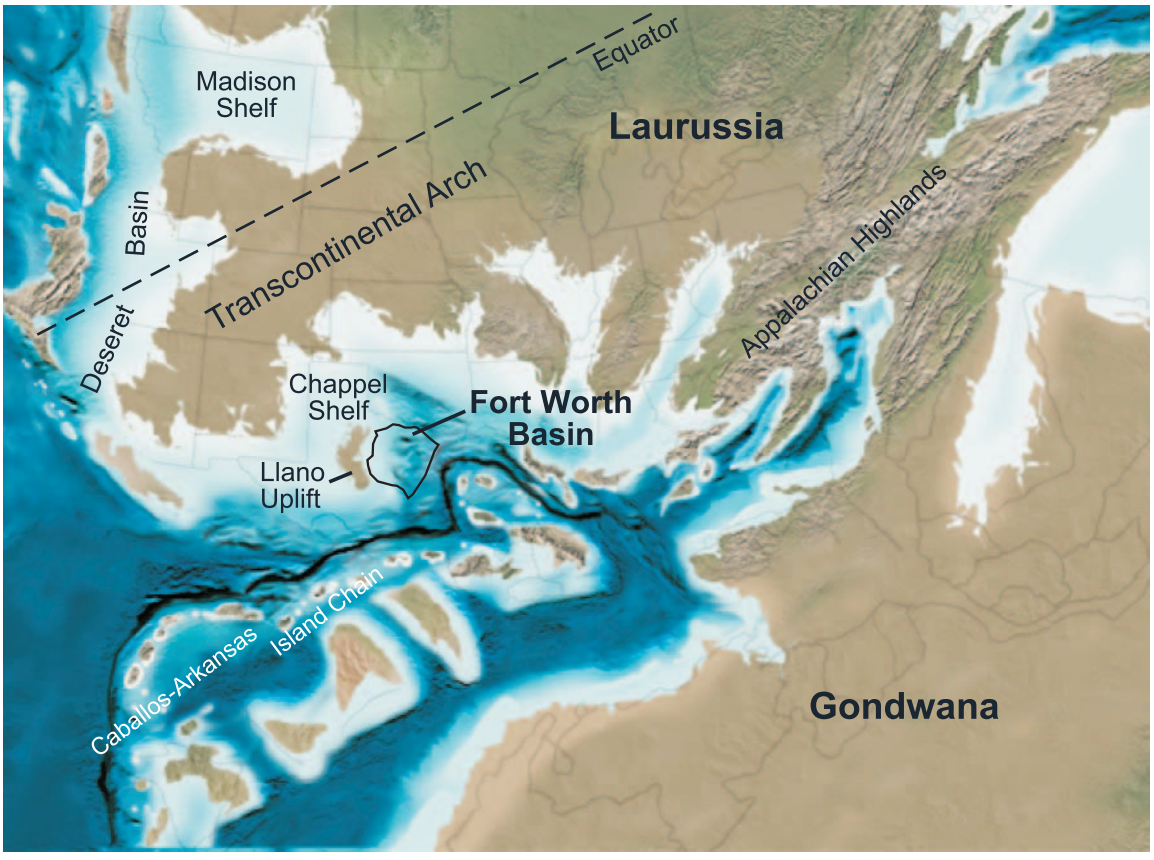

Figure 5. Regional paleogeography of the southern mid-continent region during the late Mississippian (325 Ma) showing the approximate position of the FWB. Plate reconstruction by Blakey (2005).

(180 to more than 300 m) for analogous deposits along the western margin of the craton, primarily on the basis of previously published interpretations of similar successions. Like these rocks, Barnett sediments in the FWB clearly indicate a deposition below the storm-wave base, as well as beneath an oxygen-minimum zone. Yurewicz (1977) assigned water depths of between 300 and 750 ft (90 and 230 m) to similar organic-rich mudstones of the age-equivalent Rancheria Formation in New Mexico. A modified sea level curve (Figure 7) constructed for the Lower Carboniferous section by Ross and Ross (1987) suggests that Barnett deposition occurred during a second-order, sea level highstand (Osagean to Chesterian; 320–345 Ma). Given the magnitude of the relative sea level drops (up to 150 ft [45 m]) postulated by Ross and Ross (1987), bottom depths would have to have exceeded 450 ft (140 m) to not have been affected by lowstand storm waves. This conclusion is consistent with that of Byers (1977), who assigned water depths of greater than 450 ft (140 m) to basinal anaerobic environments in which shelly fauna and bioturbation are lacking and sediment is laminated. We therefore estimate that water depths during Barnett deposition were between 400 and 700 ft (120 and 215 m). Accommodation within the FWB is probably a combination of eustatic sea level rise and crustal downwarping associated with the Ouachita orogeny.

Barnett strata of the central FWB are underlain by Ordovician carbonates (Middle to Upper Ordovician Viola-Simpson or Lower Ordovician Ellenburger strata) and overlain by the Pennsylvanian Marble Falls strata (Figure 2). Toward the west and southwest margins of the basin, the Barnett Formation is separated from the underlying Ellenburger Group by shallow-water carbonates of early Mississippian age (Chappel Formation). Ruppel (1989) interpreted the Barnett section on the west and northwest margins of the FWB to be partly time equivalent to the Chappel Formation.

Across much of the FWB, the Barnett interval can be subdivided into upper and lower sections because of the presence of the Forestburg limestone, an interval of carbonate-rich sediments.

Published and new cross sections (Figure 3) and isopach maps (Figure 4) demonstrate that the deepest

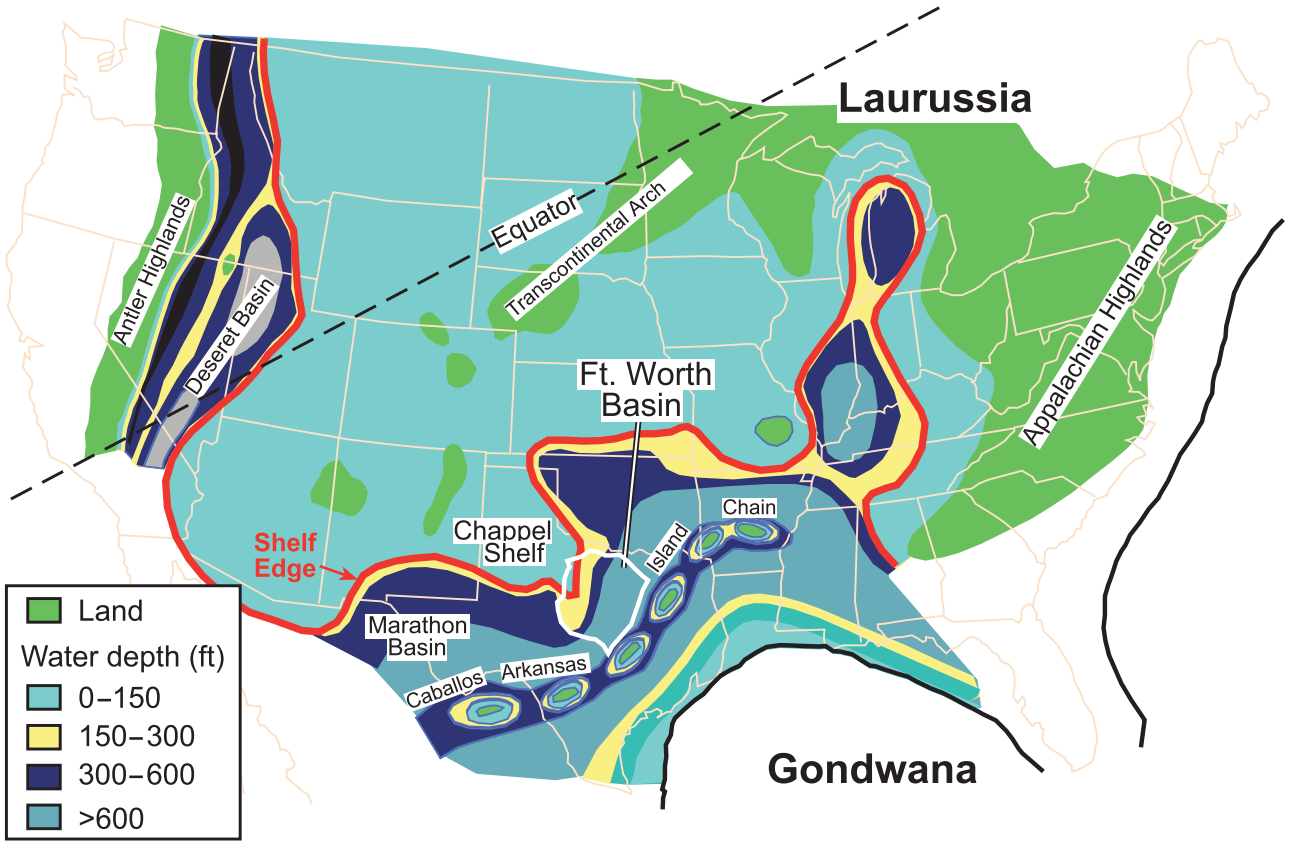

Figure 6. Middle Mississippian paleogeographic map of the United States based on studies by Gutschick and Sandberg (1983). This reconstruction suggests that the FWB was relatively deep. Modified from Gutschick and Sandberg (1983).

part of the FWB (on the basis of sediment thickness) was to the northeast. Craig and Connor (1979) and Montgomery et al. (2005) mapped more than 1000 ft (300 m) of the Barnett strata near the Muenster arch. The Forestburg limestone is also thickest on the southwest side of the Muenster arch, again indicating increasing accommodation to the northeast (Figure 4). The Barnett Formation is absent over the Muenster arch, a Pennsylvanian-age horst block, because of erosion.

LITHOFACIES

The Barnett interval comprises a variety of lithofacies, which, with the exception of skeletal debris beds, are dominated by fine-grained (clay- to silt-size) sediment. In this study, we recognize three general lithofacies on the basis of mineralogy, fabric, biota, and texture: (1) nonlaminated to laminated siliceous mudstone; (2) laminated argillaceous lime mudstone (marl); and (3) skeletal argillaceous lime packstone. Papazis (2005) described the Barnett outcrops on the Llano uplift in San Saba County, Texas, as black shale. Weathering patterns at these outcrops are consistent with true fissile shale, as defined by Folk (1980). The Barnett also contains several more minor rock types associated with concretions and hardgrounds; these units will be discussed briefly in the sections below.

Barnett facies were defined from descriptions of four cores, the most complete core section being from the Devon 7 Adams Southwest well (Figures 1, 2, 8) in Wise County. This core recovered 360 ft (110 m) of section, representing almost the entire Barnett interval extending from just below the Marble Falls contact to the Viola Limestone. Our studies of this core were based on the general core description, continuous core photographs, and thin sections presented in Papazis (2005). Two other cores from Wise County include less complete sections of the Barnett interval. The Texas United 1 Blakely core contains part of the upper Barnett section, the Forestburg limestone, and the upper part of the lower Barnett section (120 ft; 37 m) (Figures 1, 2, 9). The Mitchell Energy 2 T. P. Sims core contains only 127 ft (39 m) of the lower section of the lower Barnett interval (Figures 1, 2, 9). Covering the lowest part of the lower Barnett interval is 23 ft (7 m) of

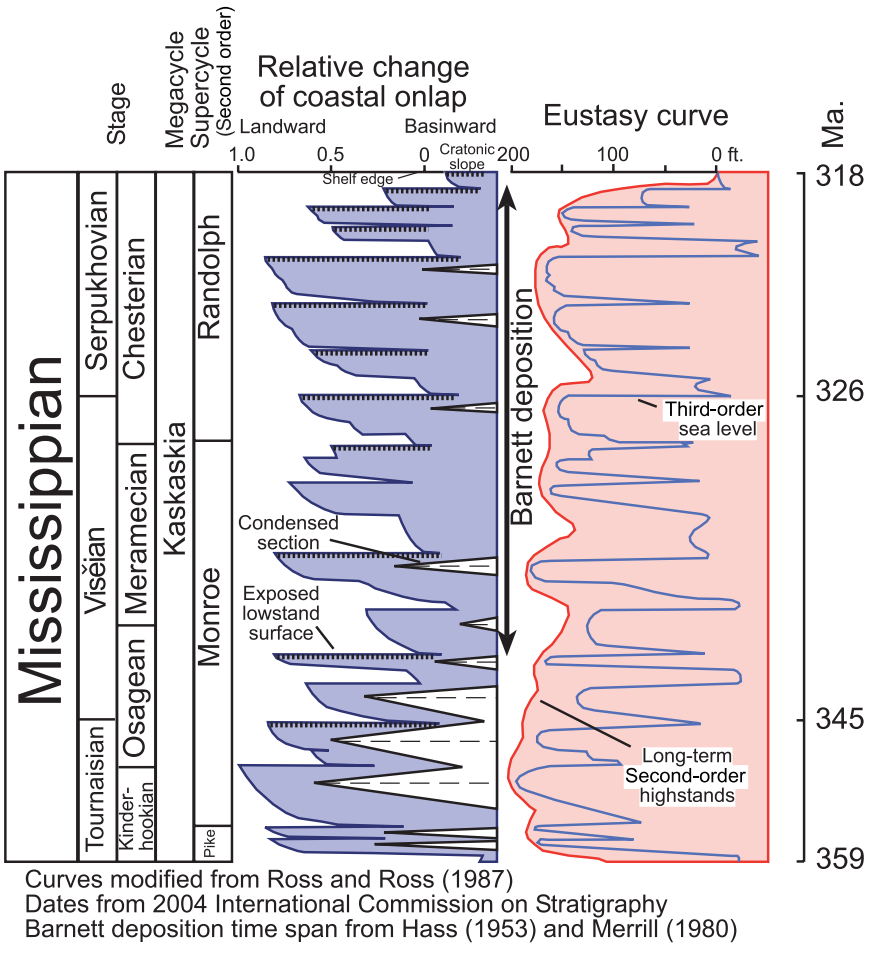

Figure 7. Plot of relative change in coastal onlap and eustasy for the Mississippian. The interval of Barnett deposition is marked.

core from the Cities Service 1 St. Clair well in Erath County (Figures 1, 2, 9).

Collectively, these cores show that the upper and lower Barnett sections are composed dominantly of a variety of siliceous mudstones with less abundant interbedded lime mudstones and skeletal packstones, whereas the Forestburg section is composed entirely of laminated, argillaceous lime mudstone. On wire-line logs (Figure 2), the Forestburg interval has a characteristic low-gamma-ray signature, attesting to its high calcite content. The Forestburg section is also very argillaceous (mean of 24%; Figure 10), but its gamma-ray response is strikingly lower than that of the adjacent high-gamma-ray Barnett siliceous mudstones.

Mineralogy and Lithology

Thin-section examination and XRD analysis (Table 1; Figure 10) show that Barnett rocks generally contain less than one-third clay minerals. According to Bowker (2002), these clays are dominantly illite with minor smectite. Silica (clay- to silt-size crystalline quartz) is by far the dominant mineral in the Barnett; carbonate (clay- to silt-size crystalline calcite and dolomite) is also locally common, along with lesser amounts of pyrite and phosphate (apatite). Carbonate in Barnett strata is mostly in the form of fossil beds. This calcite-dominated skeletal debris is locally common throughout the section (Figures 8, 9). Papazis (2005) completed a detailed analysis of Barnett mineralogy using XRD, scanning electron microscope (SEM), and microprobe analyses. Refer to the Papazis (2005) study for more detailed data on mineralogy.

The Barnett Formation in the northern FWB, not true shale, is more accurately described as a siliceous mudstone (Papazis, 2005) or, in some cases, a fine-grained siltstone. (Shale is defined as having fissility [Folk, 1980], and Barnett strata in cores from the FWB are not fissile.) Barnett rocks are commonly laminated and composed predominantly of silt-size peloids and fine skeletal debris and, in some thin units, larger skeletal material. Compaction is ubiquitous and masks some of the original texture and fabric.

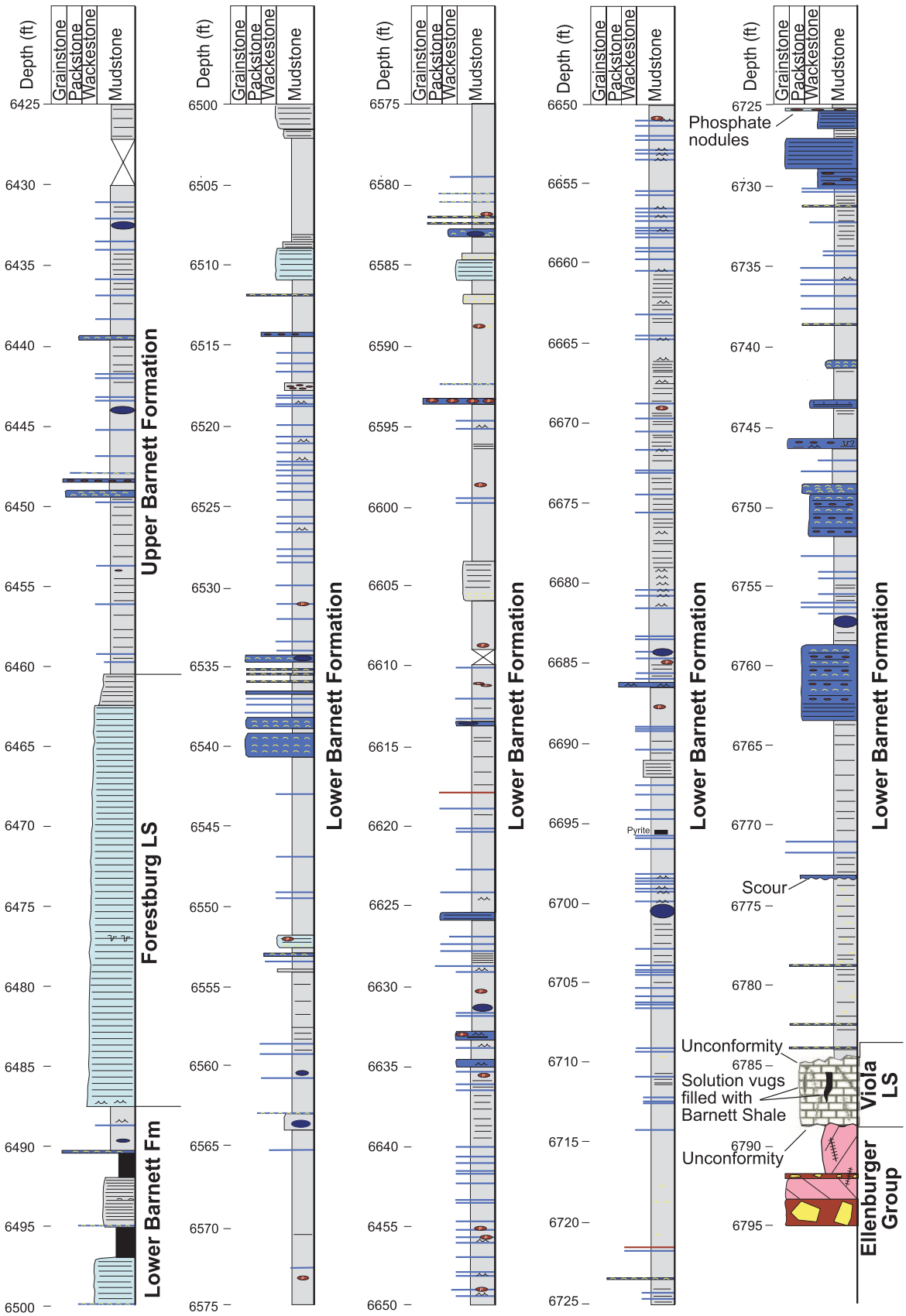

Figure 8. Lithofacies of the Devon 7 Adams Southwest core. Core description is interpreted from a figure and detailed slabbed-core and thin-section photographs by Papazis (2005). See Figure 9 for the explanation of symbols.

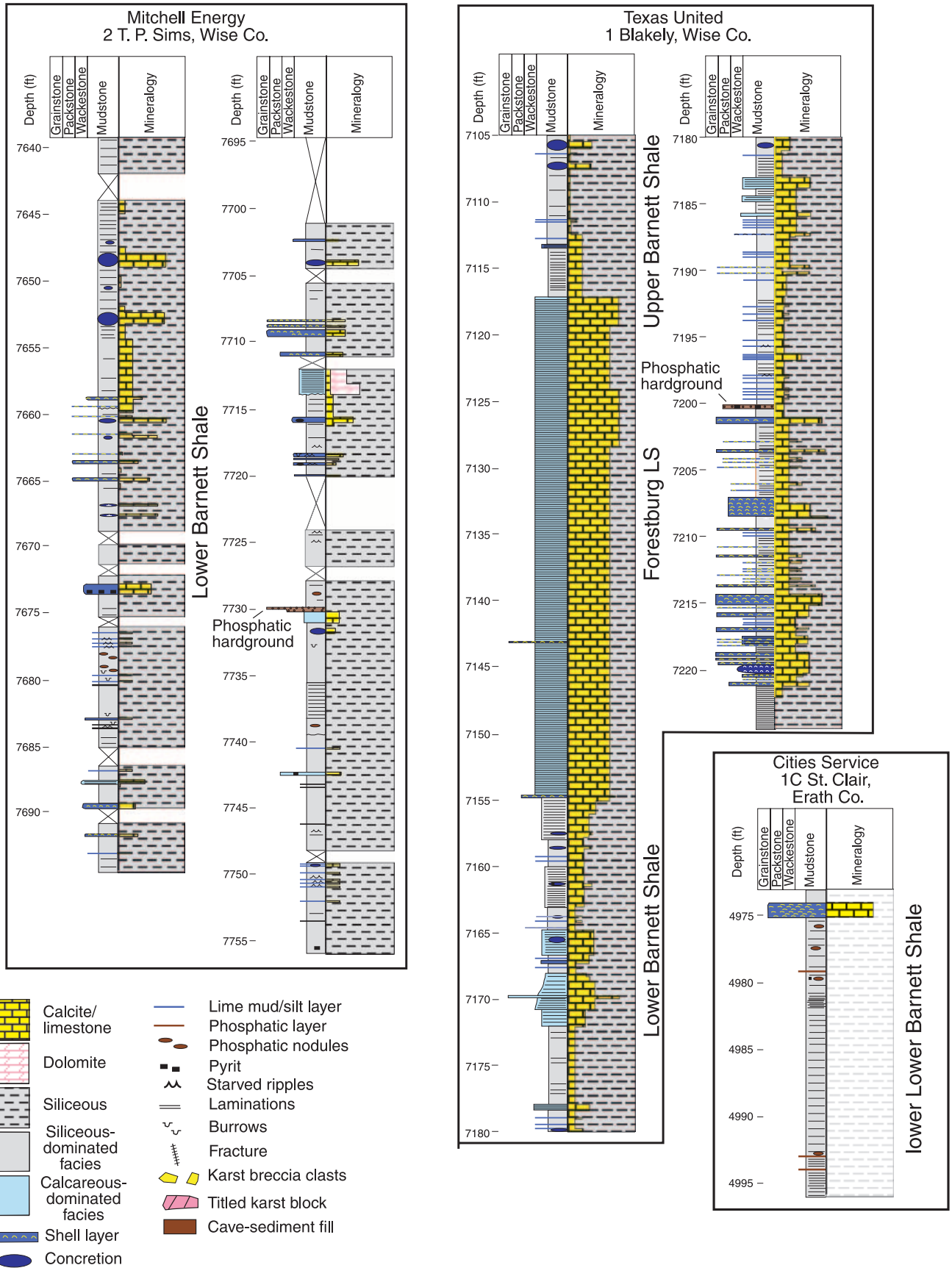

Figure 9. Descriptions of the Mitchell Energy 2 T. P. Sims, Texas United 1 Blakely, and Cities Service 1C St. Clair cores.

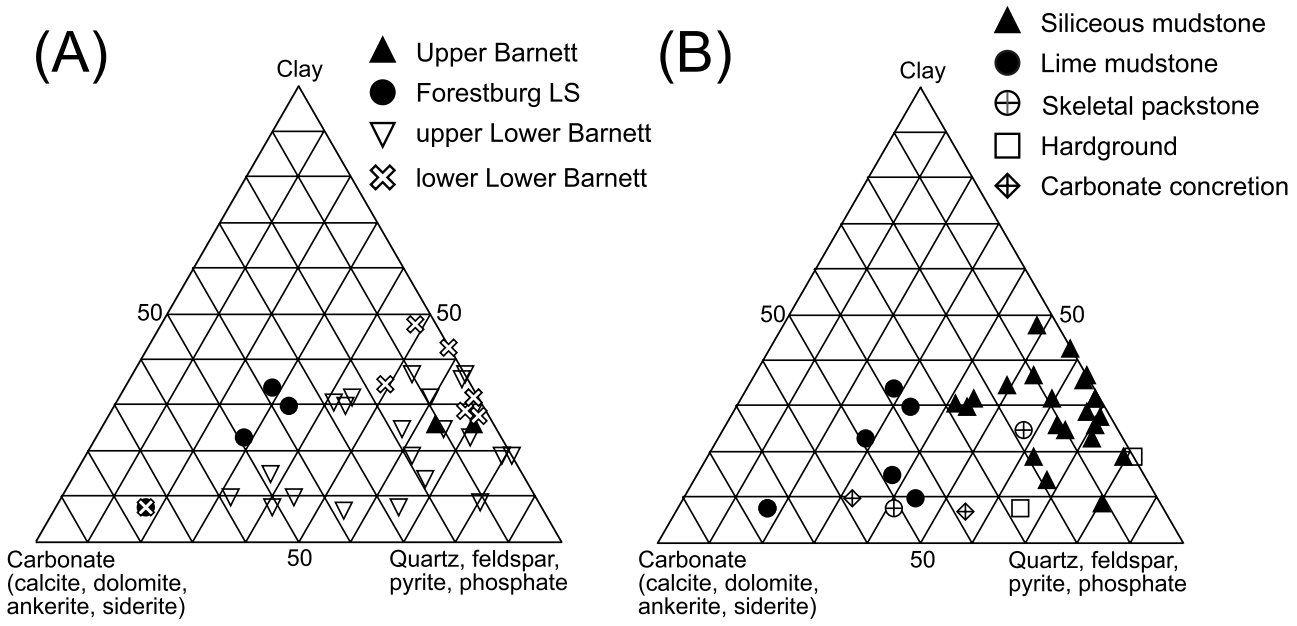

Figure 10. Ternary diagrams of Barnett mineralogy. (A) Mineralogy by member. (B) Mineralogy by lithofacies.

Ternary diagrams of Barnett mineralogical constituents show relative proportions of clay, carbonate, and other minerals (Figure 10). The Forestburg limestone contains subequal amounts of carbonate, clay, quartz, pyrite, and phosphate (Figure 10A). Barnett rocks contain less calcite than Forestburg rocks and are dominated by variable admixtures of quartz, feldspar, and other minerals. The lowermost Barnett appears to contain the least amount of carbonate and the highest amount of clay. Figure 10B and Table 1 show percentages of clay, carbonate, and other minerals for each lithofacies.

When originally deposited, Barnett strata may have contained as much as 20% total organic carbon (TOC) content (Bowker, 2003). Typical measured ranges of current TOC in the Barnett interval are between 3 and 13% (Montgomery et al., 2005). Because organic material is not defined by XRD analysis, it is not included in the bulk composition of the rock. D. Jarvie provided TOC analysis for 1 Blakely and 2 Sims cores, and the mean value of TOC for the upper Barnett is 3.9% (range: 0.4–5.2%). The Forestburg limestone averages 1.8% (range from 0.8 to 2.8%), and the upper part of the lower Barnett exhibits a mean of 4.0% (range from 1.9 to 10.6%).

Lithofacies

The Barnett Formation contains a variety of intergradational lithofacies. For the purposes of this article, we have defined three major lithofacies. X-ray analysis data show that mineralogical content ranges greatly among defined facies (Figure 10B), indicating that there is a broad spectrum of mixing among different mineralogies.

Laminated Siliceous Mudstone

Siliceous mudstone (Figure 11) is the predominant lithofacies within the upper and lower Barnett intervals, although these rocks are highly variable in character. Vertical changes from one sublithofacies to another can be sharp or gradational. Fabric ranges from nonlaminated to very well laminated. Burrows are extremely rare; only approximately five possible examples of trace fossils were observed in 630 ft (192 m) of core. Burrow traces appear to be *Helminthopsis*, *Cosmoraphe*, *Chondrites*, and *Nereites*. Each appears to have affected only a lamina or two. Two major textural components of the mudstone are silt-size peloids and fragmented skeletal material. Some (presumably softer) peloids have been reshaped by compaction into a clotted fabric. Skeletal material (Figures 11, 12) consists of radiolarians (calcite replaced), sponge spicules, filibranch mollusk fragments, cephalopods, agglutinate foraminifera (rimmed by microcrystalline quartz), conodonts, *Tasmanites* steinkerns (pelagic algal cysts), and rare echinoderm fragments. Most skeletal components are interpreted to have been transported into the deeper part of the FWB. The cephalopods, conodonts, radiolarians, and *Tasmanites* lived in the oxygenated interval of the water column.

Table 1. Mineralogical Analysis of the Barnett Formation Based on XRD Data

	Mean	Sample Count	Minimum	Maximum
Total calcite (%)	16.1	35	0	73
Siliceous mudstone: calcite (%)	5.5	22	0	19
Lime mudstone calcite (%)	39.3	7	7	73
Skeletal packstone: calcite (%)	33.0	2	15	51
Carbonate concretion: calcite (%)	37.0	2	16	58
Hardground: calcite (%)	12.5	2	0	25
Total dolomite/ankerite (%)	5.6	35	0	41
Siliceous mudstone: dolomite/ankerite (%)	3.7	22	0	14
Lime mudstone: dolomite/ankerite (%)	12.6	7	1	41
Skeletal packstone: dolomite/ankerite (%)	1.5	2	0	3
Carbonate concretion: dolomite/ankerite (%)	11.0	2	0	22
Hardground: dolomite/ankerite (%)	1.0	2	0	2
Total siderite (%)	0.3	35	0	1
Siliceous mudstone: siderite (%)	0.2	22	0	1
Lime mudstone: siderite (%)	0.7	7	0	1
Skeletal packstone: siderite (%)	0	2	0	0
Carbonate concretion: siderite (%)	0	2	0	0
Hardground: siderite (%)	0	2	0	0
Total quartz (%)	34.3	35	8	58
Siliceous mudstone: quartz (%)	41.3	22	23	58
Lime mudstone: quartz (%)	19.4	7	8	30
Skeletal packstone: quartz (%)	24.0	2	13	35
Carbonate concretion: quartz (%)	23.5	2	15	32
Hardground: quartz (%)	30.0	2	25	35
Total feldspar (%)	6.6	35	3	12
Siliceous mudstone: feldspar (%)	7.5	22	4	12
Lime mudstone: feldspar (%)	4.7	7	3	8
Skeletal packstone: feldspar (%)	4.5	2	4	5
Carbonate concretion: feldspar (%)	7.5	2	7	8
Hardground: feldspar (%)	4.5	2	4	5
Total pyrite (%)	9.7	35	1	46
Siliceous mudstone: pyrite (%)	9.4	22	1	46
Lime mudstone: pyrite (%)	4.6	7	2	9
Skeletal packstone: pyrite (%)	10.5	2	10	11
Carbonate concretion: pyrite (%)	8.5	2	8	9
Hardground: pyrite (%)	31.5	2	25	38
Total phosphate (%)	3.3	35	0	14
Siliceous mudstone: phosphate (%)	3.2	22	0	13
Lime mudstone: phosphate (%)	0.4	7	0	1
Skeletal packstone: phosphate (%)	10.0	2	7	13
Carbonate concretion: phosphate (%)	4.0	2	2	6
Hardground: phosphate (%)	7.0	2	0	14
Total clays (%)	24.2	35	7	48
Siliceous mudstone: clays (%)	29.2	22	9	48
Lime mudstone: clays (%)	18.3	7	8	34
Skeletal packstone: clays (%)	16.5	2	8	25
Carbonate concretion: clays (%)	8.5	2	7	10
Hardground clays (%)	13.5	2	8	19

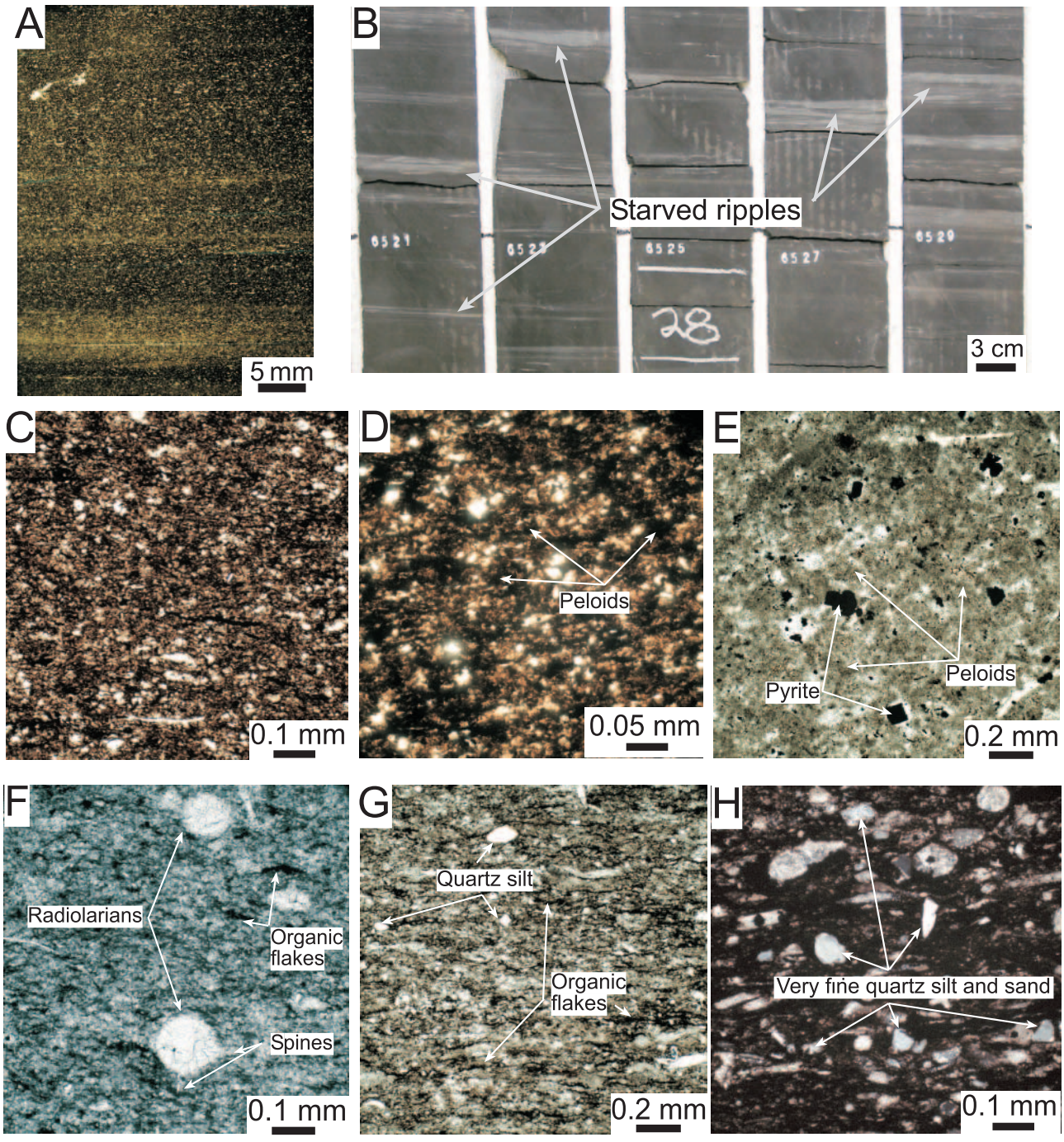

Figure 11. Photographs of siliceous mudstone lithofacies. (A) Thin section of siliceous mudstone showing faint laminae. Upper Barnett Formation: 1 Blakely, 7109 ft (2166 m). (B) Starved ripples interpreted to have formed by bottom currents. Lower Barnett Formation: 7 Adams Southwest. Core photograph from Papazis (2005). (C) Clotted peloidal texture with fossil fragments and detrital silt grains. Lower Barnett Formation: 1 Blakely, 7223 ft (2201 m). (D) Clotted peloidal texture with silt grains. Lower Barnett Formation: 2 Sims, 7223 ft (2201 m). (E) Carbonate concretion in siliceous mudstone lithofacies showing undeformed peloids. Lower Barnett Formation: 1 Blakely, 7156 ft (2181 m). (F) Calcite-replaced radiolarians with spines in organic-rich matrix (black flakes). Lower Barnett Formation: 1 Blakely, 7159 ft (2182 m). (G) Organic flakes aligned parallel to bedding. Quartz silt is also present. Lower Barnett Formation: 1 Blakely, 7164 ft (2183 m). (H) Very fine-grained quartz and skeletal debris in a thin lamina of siliceous mudstone. Lower Barnett Formation: 1 Blakely, 7156 ft (2181 m) (cross nicols).

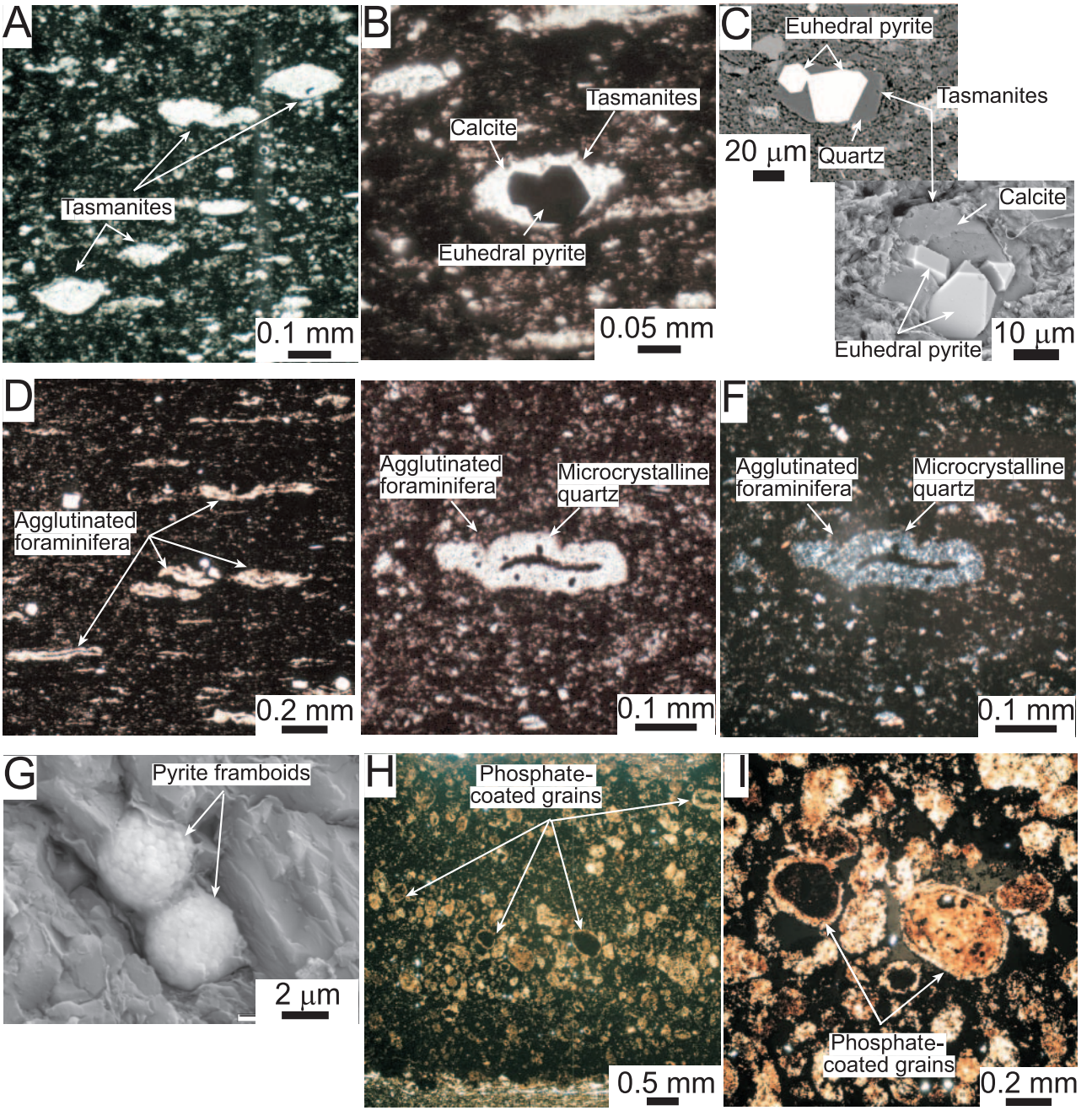

Figure 12. Photographs of siliceous mudstone lithofacies. (A) Compacted *Tasmanites* filled with calcite. Upper Barnett Formation: 1 Blakely, 7109 ft (2166 m). (B) *Tasmanites* body void filled with calcite and euhedral pyrite. Upper Barnett Formation: 1 Blakely, 7109 ft (2166 m). (C) Top: *Tasmanites* body void filled with quartz and euhedral pyrite. Scanning electron microscope photograph of thin section from Papazis (2005). Lower Barnett Formation: 2 Sims (depth unknown). Bottom: *Tasmanites* body void filled with calcite and euhedral pyrite. Scanning electron microscope photograph of rock chip. Lower Barnett Formation: 1 Blakely, 7168 ft (2184 m). (D) Flattened agglutinated foraminifera lying parallel to bedding. Lower Barnett Formation: 2 Sims, 7742 ft (2359 m). (E) Close-up of flattened, agglutinated foraminifera with microcrystalline quartz rim. Lower Barnett Formation: 2 Sims, 7745 ft (2360 m). (F) Same as (E) but under cross nicols. (G) Very fine pyrite framboids in clay and silica matrix. Lower Barnett Formation: 1 Blakely, 7168 ft (2184 m). (H) Thin (5-mm; 0.2-in.) laminae of phosphate-coated grains, peloids, and intraclasts. Lower Barnett Formation: 1 St. Clair, 4975 ft (1516 m). (I) Close-up of phosphate-coated grains shown in (H).

Detrital quartz and feldspar silt (rarely sand) are present. Organic material in the form of flakes and disseminated particles is locally abundant. Authigenic material includes silica, calcite, dolomite, pyrite (framboids and euhedral crystals), and phosphate (particulate, peloids, and coated grains). Siliceous mudstones range from calcareous to nearly totally noncalcareous. Microcrystalline quartz within the mudstone is probably a diagenetic product of opal from sponges and radiolarians (Bowker, 2003; Papazis, 2005). The diagenetically altered microcrystalline silica is a major component of the siliceous mudstone facies and is far more abundant than detrital quartz silt.

Much of the original sediment appears to have been peloidal, with the dominant size of grains in the range of 20–30 μm; some peloids range into sand size (Figure 11). Concretions (discussed in more detail below) preserve the original peloidal texture of the sediment. Thin sections of these concretions (Figure 11E) show uncompacted peloids with microspar to pseudospar cement between them. Some of this material is probably fecal pellets formed in shallower water and transported into the deeper basin. Other peloids may have been produced by flocculation of clay particles, which later settled to the sea bottom.

Compacted laminations around rigid grains suggest that up to 65% compaction has occurred. This compaction has served to enhance laminations in the mudstone, which range from continuous to discontinuous at the core scale. Some laminations are highlighted only by scattered shells, silt grains, or organic flakes. Thin, flat skeletal fragments tend to align during compaction. Organic flakes (compressed wood chips, leaf fragments, etc.) also tend to lie parallel to bedding, producing pronounced laminations. Some laminations are millimeter alternations of calcite- and clay-dominated laminae. Some laminae display millimeter-scale, fining-upward sequences, and others show scour that may be related to turbidite or contour current erosion. Ripples composed of fine silt (Figure 11B) are scattered throughout the lower Barnett interval.

Tasmanites, cysts of planktonic marine prasinophyte algae, are very common in black shale successions and contribute to the kerogen content (Greenwood et al., 2000). They have no hard parts and are generally preserved as steinkerns. Schieber (1996) and Schieber and Baird (2001) showed that early filling of *Tasmanites* tests by silica (megaquartz) and pyrite acts to preserve their original shape, although they commonly become slightly compacted (ellipsoid). Most *Tasmanites* bodies in Barnett strata are preserved as calcite steinkerns (with and without pyrite inclusions) (Figure 12A–C), although a few are preserved as quartz crystals with pyrite crystal inclusions (Figure 12C).

Agglutinate foraminifera (Figure 12D–F) in the Barnett strata, first recognized by Papazis (2005), have a microcrystalline quartz rim that was incorporated into the outer foraminiferal wall during life. Tests are compacted to flattened spheres and oriented horizontally. The foraminifera occur as isolated individuals in the mudstone or concentrated in current-deposited layers. Some of the flattened microcrystalline silica masses may actually be flattened *Tasmanites* cysts (S. T. Reed, 2006, personal communication).

The presence of detrital quartz, K-spar, and plagioclase in these rocks may be an indication of sediment sourced from the Caballos Arkansas island chain to the east (Figure 5). Northern and western areas bordering the FWB were dominated by shallow-water carbonate deposition and are unlikely sources of such immature terrigenous-derived material. Because of the apparent distance of the Caballos Arkansas island chain, it is not surprising that only the clay- and silt-size fraction of this terrigenous-derived detritus reached the Wise County area.

Pyrite is present in several forms. The most common are small framboids generally less than 10 μm in diameter; most falling into the 1–2-μm range (Figure 12G). Fine-grained framboids are commonly aggregated into larger masses. Papazis (2005) also noted an average diameter of 1 μm for these framboids. Another common form of pyrite is euhedral crystals several hundreds of micrometers in size. This form is seen as isolated crystals in *Tasmanites* steinkerns (Figure 12B, C) and in fracture fills. Pyritization of cephalopods (Figure 13G, H), bivalves (Figure 13I), concretions, and hardgrounds (Figure 14E–G) is also locally observed.

Laminated Argillaceous Lime Mudstone (Marl)

The laminated argillaceous lime mudstone facies (Figure 14A, B) is the predominant lithofacies in the Forestburg limestone. This facies is also present as thinner (<2-ft; <0.6-m) intervals in the lower Barnett section. In a weathered outcrop, this lithofacies would appear as marl. Calcite is the dominant mineral in this facies, but dolomite (in the form of 30-μm crystals) locally comprises as much as 21% of these rocks. Laminated lime mudstone is composed predominantly of lime mud and silt-size carbonate fragments. It contains up to 30% clay and up to 28% other noncarbonate minerals, such as quartz, K-spar, plagioclase, and pyrite (Figure 10B). Pyrite and phosphate, common in the

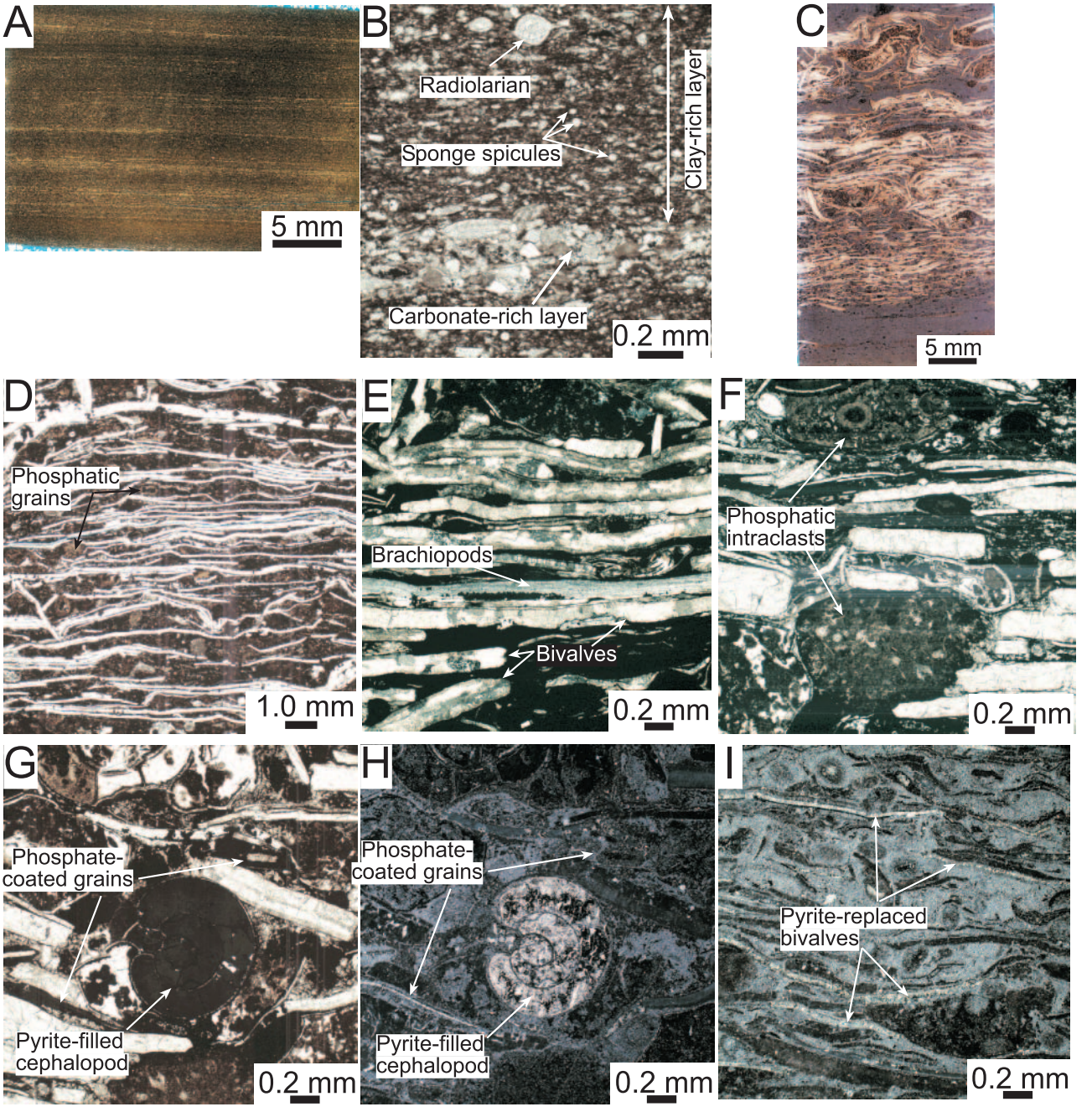

Figure 13. Photographs of argillaceous lime mudstone and skeletal packstone lithofacies. (A) Argillaceous lime mudstone showing well-developed laminae. Forestburg limestone: 1 Blakely, 7141 ft (2176 m). (B) Argillaceous-rich and argillaceous-poor laminae in argillaceous lime mudstone. Forestburg limestone: 1 Blakely, 7141 ft (2176 m). (C) Phosphate-bearing, argillaceous, skeletal packstone showing several layers of strongly compacted bivalves. Forestburg limestone: 1 Blakely, 7118 ft (2169 m). (D) Mixture of strongly compacted bivalves and phosphatic grains in skeletal packstone. Lower Barnett Formation: 2 Sims, 7708 ft (2349 m). (E) Compacted bivalves and brachiopod shells in skeletal packstone. Cross nicols. Forestburg limestone: 1 Blakely, 7118 ft (2169.5 m). (F) Phosphatic intraclasts within skeletal packstone. Forestburg limestone: 1 Blakely, 7117 ft (2169.2 m). (G) Pyrite-filled cephalopod and phosphate-coated grains in skeletal packstone. Forestburg limestone: 1 Blakely, 7117 ft (2169.2 m). (H) Same as (G), but in reflected light to emphasize pyrite. (I) Pyrite-replaced bivalves in skeletal packstone. Photograph taken in reflected light to emphasize pyrite. Forestburg limestone: 1 Blakely, 7118 ft (2169.5 m).

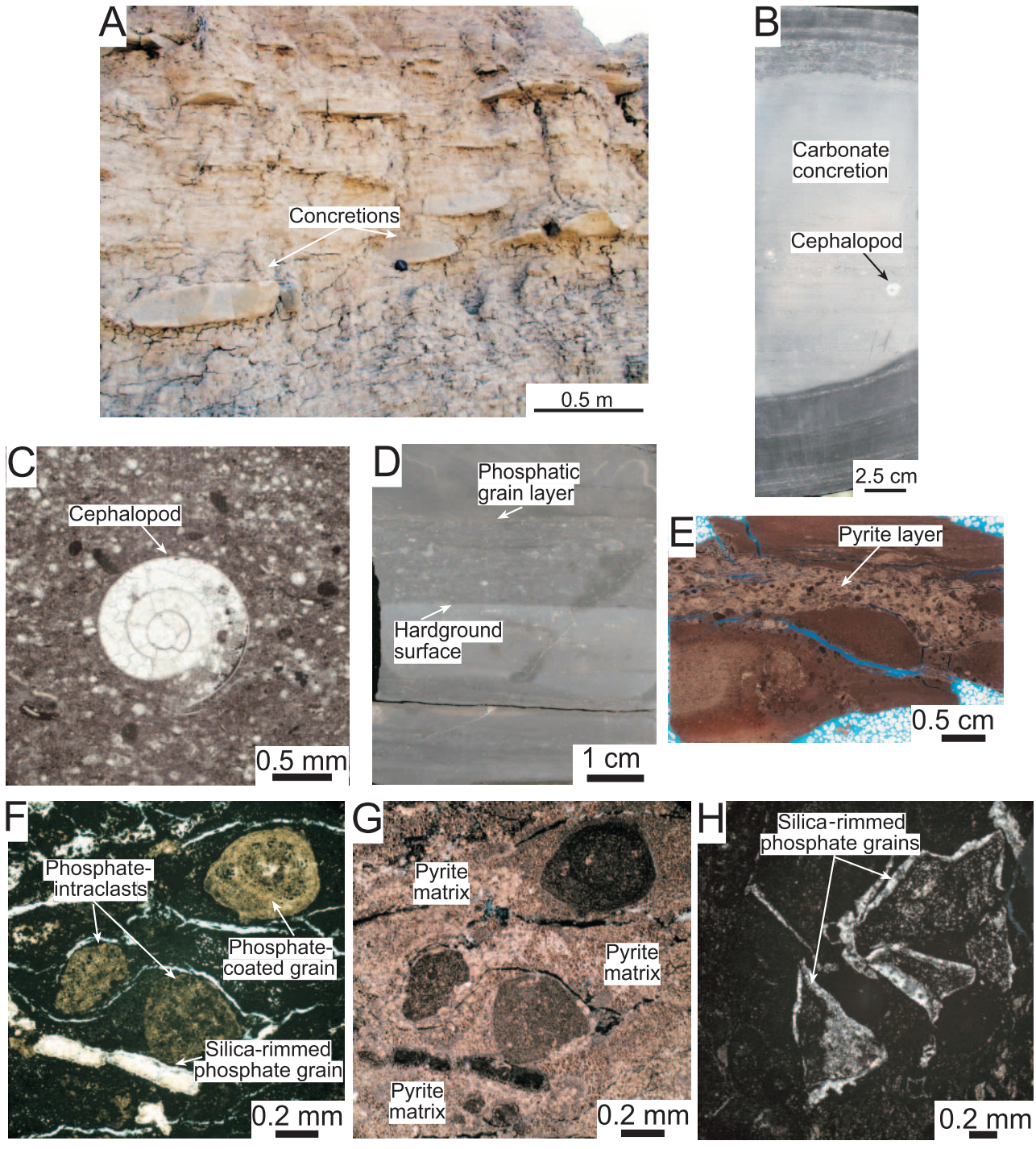

Figure 14. Photographs of concretions and hardgrounds. (A) Carbonate concretions in Barnett outcrop in San Saba County, Texas. (B) Carbonate concretion showing uncompacted bedding within the concretion and compacted siliceous mudstone laminae adjacent to the concretion. Lower Barnett Formation: 1 Blakely, 7218 ft (2200 m). (C) Close-up of concretion showing cephalopod in uncompacted fabric. Same sample as (B). (D) Polished slab of phosphatic hardground with overlying layer of phosphatic grains. Lower Barnett Formation; 2 Sims, 7730 ft (2356 m). (E) Irregular hardground composed of phosphate and pyrite. Grains include phosphate-coated grains and silica-replaced bone(?). Lower Barnett Formation; 1 Blakely, 7198 ft (2193 m). (F) Phosphate-coated grains and intraclasts in pyrite layer (dark material). Close-up of sample (E). (G) Same sample as (F), but photograph taken in reflected light to emphasize pyrite. (H) Silica replacing and rimming phosphatic bone material. Close-up of sample (E).

other two major lithofacies, are relatively rare in this lithofacies. Fossils include radiolarians, sponge spicules, and thin-walled mollusk fragments. Quartz silt is locally present, along with silt-size peloids. Laminations in these rocks are the result of interbedded layers of carbonate particles containing minor clay and carbonate particles with abundant clay (Figure 13B). Thicknesses of laminae range up to 150 μm. Laminae are emphasized by flat-lying, thin-walled mollusk fragments.

Skeletal, Argillaceous Lime Packstone

The skeletal lime packstone lithofacies is found throughout the lower Barnett interval, but it is also locally present in the upper Barnett interval (Figures 8, 9). It is not present in the Forestburg limestone. These deposits range from less than inches (tenths of a meter) to 3.5 ft (1 m) in thickness. Internally, shell layers are thin beds with thin laminae of organic-rich skeletal siliceous mudstone in between, indicating multiple events of deposition. Coarse-grained shell layers contain filibranch mollusks of various sizes, cephalopods, brachiopods, sponge spicules, and radiolarians, as well as phosphatic material.

This lithofacies is commonly rich in phosphate in the form of coated grains, intraclasts, and peloids (Table 1; mean 10%). Phosphatic debris appears to have been transported along with the shell material.

The thin shells of bivalves and cephalopods are extensively compacted (through mechanical breakage) to flattened masses (Figure 13C–F). We estimate that these units now occupy approximately 10% of their original thickness. Original matrix porosity of the mud matrix within the newly deposited shell layer is estimated to have been 70–80%. Early compaction within several feet of the surface would have decreased the mud-matrix porosity to 40–50%, decreasing the shell layer thickness by the same amount. Burial compaction promoted mechanical breakage of the thin-walled shells, producing a flattened mass of shells and mud with less than 6% porosity.

The base and top of the shell layers are irregular (Figure 13C). This irregularity is most likely produced either by compaction in which basal shells are forced into the soft mud below or by the mud above the shell layer contorting around the shells below. Note that such compaction-related features can easily be mistaken for scour.

Concretions and Hardgrounds

Calcareous concretions (Figure 14A–C) are common in the upper and lower Barnett sections in the subsurface of the FWB, as well as in outcrops. They are not, however, present in the Forestburg limestone. Concretions range in vertical thickness from less than 1 in. (2.5 cm) to 1 ft (0.3 m). In outcrops of the Barnett Formation in San Saba County, Texas, concretions are ellipsoidal, up to 1 ft (0.3 m) thick, and several feet long (Figure 14A). Internally, they preserve uncompacted bedding (Figure 14B), indicating that they formed early and prior to compaction. Beds consist of well-developed peloids (20–100 μm) and skeletal debris of mollusks cemented by microspar (<4 μm) and pseudospar (4–20 μm) (Figure 11E). Wiggins (1982) also noted diagenetic microspar within Barnett concretions. Some concretions have pyritized rims and internally contain pyrite crystals ranging from 10 to 400 μm.

Phosphate and pyrite concretions, also present, are generally only a few inches in size. Papazis (2005) noted that some of these phosphate concretions have pyrite centers. Phosphatic concretions also appear to have formed early, judging by the evidence of compaction around the margins.

Thin (<20-mm; <0.78-in.) hardground intervals (Figure 14D–H) are locally present within the lower Barnett section. Two well-developed hardgrounds were observed: one at 7730 ft (2356 m) in the 2 Sims core (Figure 14D) and one at 7198 ft (2193 m) in the 1 Blakely core (Figure 14E–H). The surfaces of both hardgrounds are phosphatic and pyritic and have phosphate-coated grains associated with them. The hardground in the 2 Sims core (Figure 14D) is phosphatic and consists of several layers. The hardground contains both diagenetic phosphate and phosphate-coated grains. Using SEM micrography, Papazis (2005) showed that the Ca phosphate is an early authigenic phase that cemented the hardground. Immediately above the hardground surface is a coarse-grained deposit of phosphatic peloids and coated grains. The 1 Blakely hardground (Figure 14E–H), more irregular than the 2 Sims hardground, has well-developed phosphate-coated grains (ooids) and massive pyrite replacement. Some phosphatic clasts (fish bone?) are replaced and rimmed by fine-crystalline quartz (Figure 14H).

DEPOSITIONAL MODEL

On the basis of sedimentary structures, facies, organic geochemistry, flora and fauna, and comparisons with regional sedimentological and tectonic features, we propose a model (Figure 15) that accounts for depositional and diagenetic processes and products observed in the

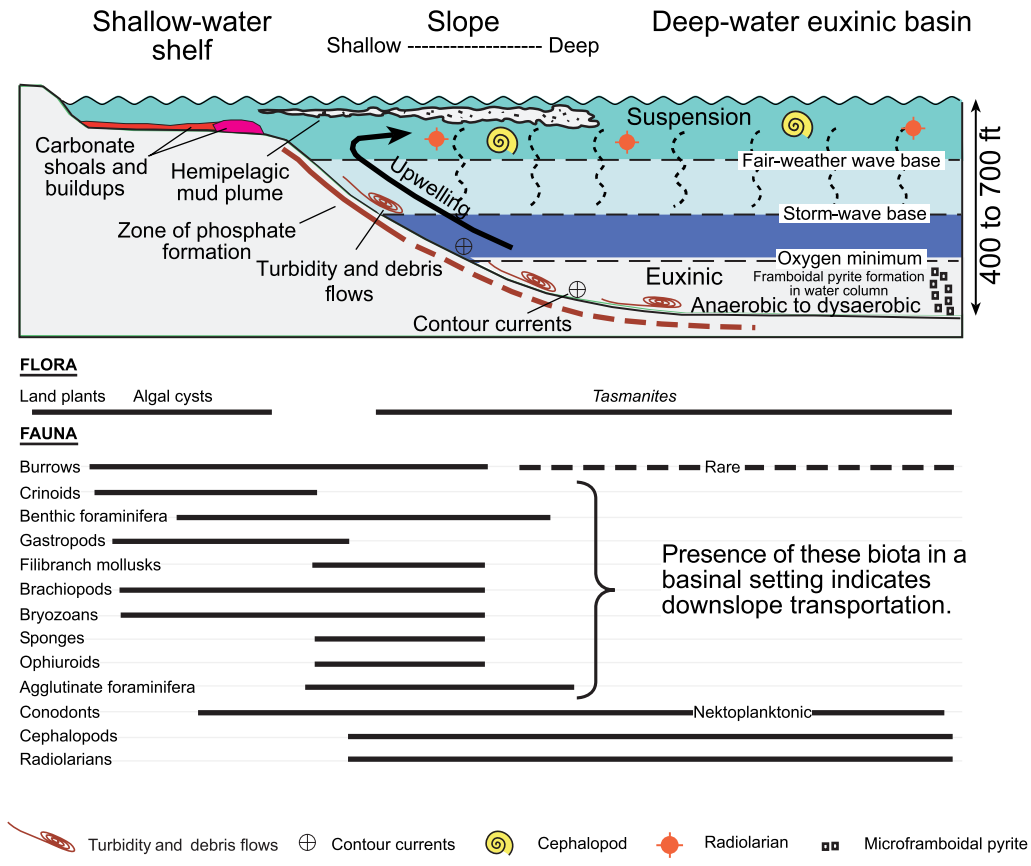

Figure 15. Generalized model for the Barnett Formation showing depositional profile, depositional processes, and estimated distribution of biota. Most of the FWB is interpreted to have been generally euxinic, except during short periods of event deposition, when hyperpycnal flow carried oxygenated water into the basin.

Barnett Formation. We think that the Barnett depositional facies in the central FWB are most appropriately interpreted as having formed in a deep-water slope-to-basinal setting. The basin was characterized by dysaerobic to anaerobic bottom conditions developed below storm-wave base and below the oxygen minimum zone. Sedimentation in the basin was primarily the result of two processes: suspension settling and density currents. This interpretation is consistent with evidence and models presented by other workers in many analogous settings (Byers, 1977; Yurewicz, 1977; Gutschick and Sandberg, 1983). Evidence also exists that sediment occasionally was locally reworked by contour currents. Although faunal and floral fossils are common in the Barnett strata, we think that these are dominantly transported from adjacent shelves and upper-slope settings.

Depositional Setting and Processes

As discussed earlier, regional data (Figures 5, 6) indicate that the FWB occupied a long, narrow, deeper water foreland basin that was poorly connected to the open ocean. The shape of the basin and its limited interconnection with open oceans most likely produced water-column stratification.

Major depositional processes inferred from Barnett facies and sedimentary structures include suspension settling, turbidity currents, debris flows, and contour currents. Both laminated siliceous mudstone and laminated lime mudstone formed dominantly from suspension settling. Evidence of this process includes fine laminations, fine grain size, and scarcity of larger skeletal debris. The material in these suspension sediments most likely came from two major sources: hemipelagic mud plumes transported from the shallow-water shelf and skeletal tests from within the water column.

Clay-size and very fine, silt-size particles (siliceous and carbonate) could have been transported into the basin by mud plumes associated with storm return, hypopycnal flow associated with deltas (Bates, 1953), or by less dense shelf water spreading over an intermediate dense fluid layer in a stratified basin (Harms, 1974). Clay-size material can flocculate within the water column to form peloids (Boggs, 1987), which settle to the sea bottom more quickly than individual clay particles. As noted earlier, peloids are common in the Barnett lithofacies. Basin upwelling (proposed by

Gutschick and Sandberg, 1983) may have created algal blooms that would also have contributed to suspension sedimentation. Upwelling may also have promoted blooms of radiolarians and contributed to phosphate grain development on the slope (Parrish, 1999; Lazurus, 2005). Many of the laminae present in the Barnett facies are composed of both extrabasinal material, such as clay and quartz and feldspar silt, and intrabasinal material, such as carbonate debris from the shelf and slope and carbonate organisms that lived in the oxic water column. All of these sediment particles indicate transportation from shallower water sources to the deeper basin floor. A likely mechanism for transport from the shelf and slope is dilute turbidity currents, which can carry fine-grained material similar to that in the Barnett interval, several hundred miles into a basin (Mulder and Alexander, 2001). Every turbidity current event can deposit thin units ranging from less than 1 mm (0.04 in.) to a few centimeters. No Barnett lithofacies shows divisions of the Bouma turbidite sequence. This lack of Bouma turbidite features and the dominantly fine grain size of Barnett facies are consistent with deposition occurring at great distances from the sediment source. By the time turbidity currents reached the Wise County area, most of the coarser grained material had dropped out of the flow, leaving only fine-grained sediment to be deposited in these deeper and more distal parts of the basin.

Barnett skeletal lime packstones are best interpreted as debris flows. The skeletal debris (mainly thin-shelled filibranch mollusks and brachiopods) was probably transported from the upper slope, in mud-matrix–rich flows. The delicate, thin shells were supported by buoyancy and fluid pressure of the mud matrix (Mulder and Alexander, 2001). The phosphatic material was probably incorporated in the flow from the area of the slope or within the basin. After deposition, these debris-flow beds underwent compaction, perhaps as much as 90% of their original thickness; the debris flows must have originally been very thin. With the present thickness of each event bed being less than 1 in. (2.54 cm), original depositional thickness could not have been more than 1 ft (0.3 m). Such thin event beds are further evidence of long-distance transport of the debris flow.

Scattered throughout the lower Barnett interval are very low-angle, starved ripples composed of siliceous, carbonate, and more rarely phosphatic silt (Figure 11B). These ripples are typically grouped in sets of less than 1 in. (2.54 cm). It appears unlikely that these isolated ripples are related to turbidity currents. Instead, we interpret these starved ripples to have formed by contour currents that locally reworked the sea bottom. Strong contour currents can be present in deep basins. Stow et al. (2002) reported that contour currents commonly attain velocities of 10–20 cm/s (4–8 in./s), but velocities can exceed 1–2 m/s (3.3–6.6 ft/s). They also noted that these currents can erode, transport, and deposit sediments in the range of clay to fine-sand grades and even coarser material, such as sands and gravels.

Some laminations observed in Barnett rocks may also be the result of contour currents. Sivkov et al. (2002, their figure 10) illustrated core samples from a modern, shallow-water (about 750-ft [230-m]-deep) contourite system in the Baltic Sea that contain fine-scale laminae resulting from small variations in organic carbon content. These contourite sediments consist of flocculated, marine, sapropelitic silty clay or clayey silt. Bioturbation is rare, and sediments containing patches of iron monosulfide are similar to Barnett laminated siliceous mudstone lithofacies.

The phosphatic hardgrounds found within the Barnett section are also indicative of deposition in deeper water. They document hiatuses caused by episodes of nonsedimentation (Schlager, 1998). Such hardgrounds, and the hiatuses they represent, are common features of sedimentary successions characterized by episodic transport and settling of fine-grained allochthonous sediment into distal, deeper water basins. The Barnett was deposited over a 25-m.y. period, which represents a sediment average accumulation rate of approximately 14 μm/yr. Given this low rate of sedimentation, it is not surprising that several periods of hardground development occurred.

Biota

No evidence exists in Barnett cores of any living biota in the deeper part of the FWB. The near absence of bioturbation and the laminated bedded character of the skeletal debris indicate that these faunal elements were transported into the area. We suggest that all benthic biota were confined to the shallow-water shelf or to the slope above an oxygen-minimum zone, which is the likely living area for filibranch mollusks, brachiopods, and agglutinating foraminifera. Pelagic fauna also lived in the oxygenated water column and accumulated on the sea floor after death. The rare burrows noted within the Barnett strata are associated with event deposition, indicating that organisms were transported into the deeper basin, where they were unable to colonize the muddy substrate.

Pyrite Framboid Genesis

As already noted, several forms of pyrite are present in the Barnett Formation. Pyrite framboids have been cited as a key to understanding water-column chemistry in ancient strata (Wilkin et al., 1996, 1997; Hawkins and Rimmer, 2002; Bond et al., 2004). Wilkin et al. (1996, p. 3897) stated that ''where secondary pyrite growth is limited, as to preserve primary pyrite textures, framboid size distribution may be used to indicate whether fine-grained sedimentary rocks were deposited under oxic or anoxic conditions.'' They noted that the size of framboids in modern Black Sea sediments is related to chemical conditions of the water from which they precipitate. Very fine pyrite framboids (mean 5 μm; range 1–18 μm) are typically associated with deposition from a euxinic (anoxic and sulfidic) water column, whereas larger framboids (mean 10 μm; range 1–50 μm) are associated with oxic conditions (Wilkin et al., 1997). After precipitation in the euxinic water column, the framboids settle to the sea bottom and cease to grow because of the exhaustion of reactive iron. Hawkins and Rimmer (2002) and Bond et al. (2004) have correlated very fine pyrite framboids with paleoredox conditions in ancient strata. Hawkins and Rimmer (2002) equated the presence of very fine framboids to euxinic conditions during the deposition of organic-rich black shale units in the Devonian–Mississippian section of central Kentucky. Bond et al. (2004) recognized these very fine framboids from strata deposited during marine anoxia events of the Late Devonian in Europe. The dominant, small size (~1 μm) of the framboids in the Barnett strata, therefore, suggests precipitation from a euxinic water column, which is in agreement with the absence of in-place biota, high TOC, and laminated sediment.

Total Organic Content

The Barnett interval is a super-rich source rock, with TOC ranging from 3 to 13% (Montgomery et al., 2005). High TOC indicates an anoxic setting in which bacteria that typically attack and destroy organic matter are absent. The abundance of organic matter indicates that the Barnett sea bottom was generally anoxic, for if the sea bottom had been aerobic, bacteria would have thrived and consumed much of the organic material. In an aerobic setting, bioturbation would also have been common, and sediment laminations would have been obliterated. Barnett strata took approximately 25 m.y. to be deposited, indicating a slow sedimentation rate (starved basin). The organic material probably could not have accumulated fast enough over this period to have suppressed bacterial degradation or bioturbation. Assuming an uncompacted average thickness of 1100 ft (325 m) (the present-day average thickness of the Barnett section in Wise County is 550 ft [168 m], Figure 4A, and the muddy sediments were compacted at least 50%) and a 25-m.y. time span for deposition (Figure 7), the sedimentation rate averaged 14 μm/yr. In an aerobic environment, this rate of sedimentation is far too low to prevent bacterial activity and bioturbation processes from occurring. Sedimentation, however, is commonly not uniform over time. One could interpret each lamination as an event bed (deposited instantaneously relative to geologic time), with each lamination averaging 1 mm (0.04 in.) in thickness. In this scenario, each punctuated depositional event would have been separated from previous and following events by about 150 yr (assuming a uniform frequency during the 25-m.y. interval). Again, this period would seem to be ample time for bacterial degradation of organic material to occur under aerobic conditions.

Discussion

Our data and observations suggest a deeper water setting for the Barnett strata in the northern FWB. No evidence exists that sedimentation occurred above the storm-wave base, and there is an abundance of evidence that sedimentation occurred under anoxic conditions. Inferred depositional processes and distribution of biota suggest downslope transport of biotic elements from shallower water areas; no biota appear to be in situ. Lack of bioturbation and high TOC are strong evidence of anoxic bottom conditions. The presence of fine-grained pyrite framboids supports a euxinic water column. Integrating this evidence with the regional depositional setting of the FWB and comparing the Barnett Formation with similar successions in other starved Mississippian basins (Gutschick and Sandberg, 1983), we suggest that water depths may have been as great as 400–700 ft (120–210 m). These depths seem required for below storm-wave base and stratified water-column conditions. Barnett deposition was remarkably uniform over a 25-m.y. period, suggesting a deeper water setting in which conditions remained relatively unchanging. In a shallower setting, the sea bottom would have been periodically reached by storm-generated waves, especially during lowstands of relative sea level. No evidence exists within the Barnett sediments of any storm-wave reworking.

Because of its high calcite content, the Forestburg limestone is perhaps the most unusual deposit within the Barnett succession. However, Forestburg facies, sedimentary structures, and biota (except for the absence of large bivalves) are similar to those observed in the more typical Barnett strata (upper and lower members). This similarity demonstrates that, although more calcareous, Forestburg strata were deposited under similar conditions. The abundance of carbonate in Forestburg mudstones may reflect a change in source area, sea level rise, or seawater chemistry or circulation. In addition to higher carbonate content, the Forestburg section contains much less silica (quartz) than other parts of the Barnett Formation, indicating a change in upwelling rate brought on by a change in circulation. However, it seems more likely that Forestburg sediments represent a change to a more carbonate-dominated sediment source, perhaps associated with sea level rise and possibly faster rates of deposition. A probable source area for carbonate sediment is the western margin of the FWB (the Bend arch). During sea level rise (transgression), sediment supply from major terrigenous source areas may have been diminished. Sea level rise would also result in source areas being more distant from the FWB, which would explain the near absence of larger skeletal debris. Note that the eustatic sea level curve in Figure 7 shows a large-scale transgression during the Chesterian stage, which could have affected the upper Barnett Formation (Forestburg) deposition. Forestburg mudstones may thus represent the transport of fine-grained shelf carbonate debris by dilute turbidity flow and suspension processes. The reduced volume of silica in Forestburg rocks suggests that rates of carbonate deposition may have been somewhat higher than those indicated for deposition of Barnett siliceous muds. As discussed previously, the Forestburg limestone contains only half the TOC of lower or upper Barnett members, perhaps another indication of shelf flooding and reduced supply of organic matter to the basin. Alternatively, faster rates of deposition could also lead to lower volumes of TOC volumes.

CONCLUSIONS

The Mississippian Barnett Formation in the FWB is composed predominantly of calcareous siliceous mudstone and argillaceous lime mudstone, with intercalated thin beds of skeletal debris. It was deposited over a 25-m.y. time span in a deeper water foreland basin that had poor circulation with the open ocean. For most of the basin's history, bottom waters were euxinic, preserving organic matter and, thus, producing an organic-rich source rock. Microframboids of pyrite precipitated from this euxinic water column, and anoxic bottom conditions prohibited bioturbation. Most biota within the basin were transported from adjacent shelves or from oxygenated upper-slope environments by hemipelagic mud plumes, dilute turbidites, and debris flows. Sediment was also sourced from the oxygenated water column. Radiolarians living in the water column and siliceous sponge spicules transported from the slope were likely the primary source of silica in the mudstones. The dearth of coarser grained terrigenous-derived material (sand) is an indication of the great distance from terrigenous source areas.

Available evidence shows that Barnett strata in the FWB were deposited in a deeper water, euxinic, foreland basin well below the storm-wave base. No evidence exists that sediments were reworked by shallow-water processes. All sedimentological features can be attributed to suspension, density-flow, and contour-current processes.

REFERENCES CITED

Arbenz, J. K.,1989, The Ouachita system, *in* A. W. Bally and A. R. Palmer, eds., The geology of North America— An overview: Geological Society of America, The Geology of North America, v. A, p. 371–396.

Bates, C. C., 1953, Rational theory of delta formation: AAPG Bulletin, v. 37, p. 2119–2162.

Blakey, R., 2005, Paleogeography and geologic evolution of North America; images that track the ancient landscapes of North America: http://jan.ucc.nau.edu/~rcb7/nam.html (accessed September 8, 2006).

Boggs, S. Jr., 1987, Principles of sedimentology and stratigraphy: Columbus, Ohio, Merrill Publishing Co., 784 p.

Bond, S., P. B. Wignall, and G. Racki, 2004, Extent and duration of marine anoxic during the Frasnian–Famennian (Late Devonian) mass extinction in Poland, Germany, Austria and France: Geological Magazine, v. 141, p. 173–193.

Bowker, K. A., 2002, Recent developments of the Barnett Shale play, Fort Worth Basin, *in* B. E. Law and M. Wilson, eds., Innovative Gas Exploration Concepts Symposium: Rocky Mountain Association of Geologists and Petroleum Technology Transfer Council, October, Denver, Colorado, 16 p.

Bowker, K. A., 2003, Recent developments of the Barnett Shale play, Fort Worth Basin: West Texas Geological Society Bulletin, v. 42, p. 4–11.

Brown, D., 2006, Barnett may have Arkansas cousin: AAPG Explorer, v. 27, no. 2, p. 8 and 10.

Byers, C. W., 1977, Biofacies patterns in euxinic basins: A general model, *in* H. E. Cook and P. Enos, eds., Deep-water carbonate environments: SEPM Special Publication 25, p. 203–219.

Craig, L. C., and C. W. Connor, coordinators, 1979, Paleotectonic investigations of the Mississippian system in the United States: U.S. Geological Survey Professional Paper 1010, p. 371–406.

Curtis, J. B., 2002, Fractured shale-gas systems: AAPG Bulletin, v. 86, p. 1921–1938.

Durham, L. S., 2005, Barnett Shale play still going strong: AAPG Explorer, May, p. 4–6.

Folk, R. L., 1980, Petrology of sedimentary rocks: Austin, Texas, Hemphill Publishing Co., 182 p.

Gonzalez, R., 2004, A GIS approach to the geology, production, and growth of the Barnett Shale play in Newark East field: Master's thesis, University of Texas at Dallas, Dallas, Texas, POEC 6386, 24 p., http://www.searchanddiscovery.net/documents/2005/gonzalez/index.htm.

Greenwood, P. F., K. R. Arouri, and S. C. George, 2000, Tricyclic terpenoid composition of *Tasmanites* kerogen as determined by pyrolysis GC-MS: Geochimica et Cosmochimica Acta, v. 64, p. 1249–1263.

Gutschick, R., and C. Sandberg, 1983, Mississippian continental margins on the conterminous United States, *in* D. J. Stanley and G. T. Moore, The shelf break: Critical interface on continental margins: SEPM Special Publication 33, p. 79–96.

Harms, J. C., 1974, Brushy Canyon, Texas: A deep-water density current deposit: Geological Society of America Bulletin, v. 85, p. 1763–1784.

Hass, W. H., 1953, Conodonts of Barnett Formation of Texas: U.S. Geological Survey Professional Paper 243-F, p. 69–94.

Hawkins, S., and S. M. Rimmer, 2002, Pyrite framboid size and size distribution in marine black shales: A case study from the Devonian–Mississippian of central Kentucky (abs.): North-Central Section (36th) and Southeastern Section (51st), Geological Society of America Joint Annual Meeting, April 3–5, 2002, Paper No. 26-0, http://gsa.confex.com/gsa/2002NC/finalprogram/abstract_33092.htm (accessed August 25, 2006).

Henry, J. D., 1982, Stratigraphy of the Barnett Shale (Mississippian) and associated reefs in the northern Fort Worth Basin, *in* C. A. Martin, ed., Petroleum geology of the Fort Worth Basin and Bend arch area: Dallas Geological Society, p. 157–178.

Lazurus, D., 2005, A brief review of radiolarian research: Paläontologische Zeitschrift, v. 79, no. 1, p. 183–200.

Merrill, G. K., 1980, Preliminary report on the restudy of conodonts from the Barnett Formation, *in* D. Windle, ed., Geology of the Llano region, central Texas: West Texas Geological Society Publication 80-73, p. 103–107.

Montgomery, S. L., 2004, Barnett Shale: A new gas play in the Fort Worth Basin: IHS Energy Petroleum Frontiers, v. 20, no. 1, 74 p.

Montgomery, S. L., D. M. Jarvie, K. A. Bowker, and R. M. Pollastro, 2005, Mississippian Barnett Shale, Fort Worth Basin, north-central Texas: Gas-shale play with multi-trillion cubic foot potential: AAPG Bulletin, v. 89, p. 155–175.

Mulder, T., and J. Alexander, 2001, The physical character of subaqueous sedimentary density flows and their deposits: Sedimentology, v. 48, p. 269–299.

Papazis, P. K., 2005, Petrographic characterization of the Barnett Shale, Fort Worth Basin, Texas: Master's thesis, University of Texas at Austin, Austin, Texas, 142 p., CD-ROM (SW0015), available from Bureau of Economic Geology, University of Texas at Austin.

Parrish, J. T., 1999, Interpreting pre-Quaternary climate from the geologic record: Perspectives, *in* D. J. Bottjer and R. K. Bambach, eds., Paleobiology and Earth History Series: New York, Columbia University Press, 338 p.

Ross, C. A., and J. R. P. Ross, 1987, Late Paleozoic sea levels and depositional sequences, *in* C. A. Ross and D. Haman, eds., Timing and deposition of eustatic sequences: Constraints on seismic stratigraphy: Cushman Foundation for Foraminiferal Research Special Publication 24, p. 137–149.

Ruppel, S. C., 1985, Stratigraphy and petroleum potential of pre-Pennsylvanian rocks, Palo Duro Basin, Texas Panhandle: University of Texas at Austin Bureau of Economic Geology Report of Investigations 147, 81 p.

Ruppel, S. C., 1989, Summary of Mississippian stratigraphy in north and north-central Texas, *in* C. E. Mear, C. L. McNulty, and M. E. McNulty, eds., A Symposium on the Petroleum Geology of Mississippian Carbonates in North-Central Texas: Fort Worth Geological Society and Texas Christian University, p. 49–55.

Schieber, J., 1996, Early diagenetic silica deposition in algal cysts and spores: A source of sand in black shales?: Journal of Sedimentary Research, v. 66, p. 175–183.

Schieber, J., and G. Baird, 2001, On the origin and significance of pyrite spheres in Devonian black shales of North America: Journal of Sedimentary Research, v. 71, p. 155–166.

Schlager, W., 1998, Exposure, drowning and sequence boundaries on carbonate platforms, in G. F. Camoin and P. J. Davies, eds., Reefs and carbonate platforms in the Pacific and Indian oceans: International Association of Sedimentologists Special Publication 25, p. 3–21.

Sivkov, V., V. Gorbatskiy, A. Kuleshov, and Y. Zhurov, 2002, Muddy contourites in the Baltic Sea: An example of a shallow-water contourite system, *in* D. A. V. Stow, C. J. Pudsey, J. A. Howe, J.-C. Faugères, and A. R. Viana, eds., Deep-water contourite systems: Modern drifts and ancient series, seismic and sedimentary characteristics: Geological Society (London) Memoir 22, p. 121–136.

Stow, D. A. V., J.-C. Faugères, J. A. Howe, C. J. Pudsey, and A. R. Viana, 2002, Bottom currents, contourites and deep-sea sediment drifts: Current state of the art, *in* D. A. V. Stow, C. J. Pudsey, J. A. Howe, J.-C. Faugères, and A. R. Viana, eds., Deep-water contourites systems: Modern drifts and ancient series, seismic and sedimentary characteristics: Geological Society (London) Memoir 22, p. 7–20.

Turner, G. L., 1957, Paleozoic stratigraphy of the Fort Worth Basin, *in* Abilene and Fort Worth Geological Societies Joint Field Trip Guidebook: Abilene Geological Society, Fort Worth Geological Society, p. 57–77.

Wiggins, W. D., 1982, Depositional history and microspar development in reducing pore water, Marble Falls Limestone (Pennsylvanian) and Barnett Shale (Mississippian), central Texas: Ph.D. dissertation, University of Texas at Austin, Austin, Texas, 159 p.

Wilkin, R. T., H. L. Barnes, and S. L. Brantley, 1996, The size distribution of framboidal pyrite in modern sediments: An indicator of redox conditions: Geochimica et Cosmochimica Acta, v. 60, p. 3897–3912.

Wilkin, R. T., M. A. Arthur, and W. E. Dean, 1997, History of water-column anoxia in the Black Sea indicated by pyrite framboids size distributions: Earth and Planetary Science Letters, v. 148, p. 517–525.

Williams, P., 2006, New shale-gas play unfolding: Oil and Gas Investor, January 2006, supplement, p. 18–20.

Yurewicz, D. A., 1977, Sedimentology of Mississippian basin-facies carbonates, New Mexico and west Texas— The Rancheria Formation, *in* H. E. Cook and P. Enos, eds., Deep-water carbonate environments: SEPM Special Publication 25, p. 203–219.